Modeling of the diffuse ISM dynamics and chemistry

B. Godard, G. Pineau des Forêts, P. Hennebelle

E. Bellomi, S. Bialy, M. Pérault,

V. Valdivia, P. Lesaffre

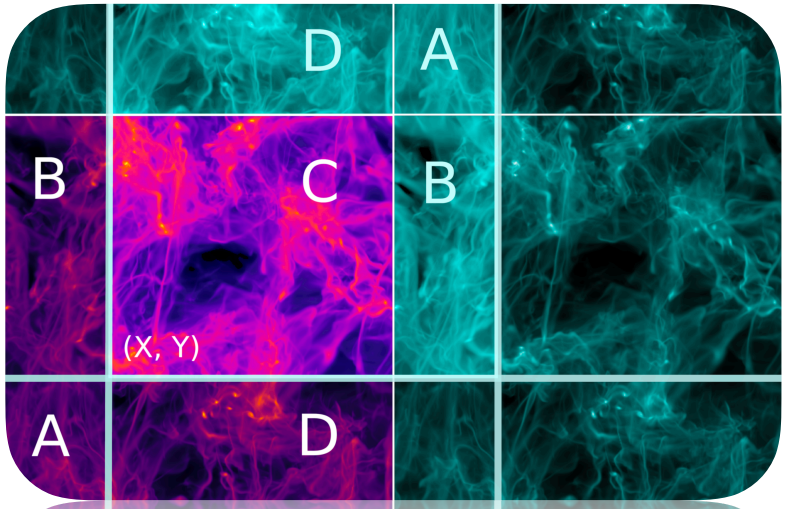

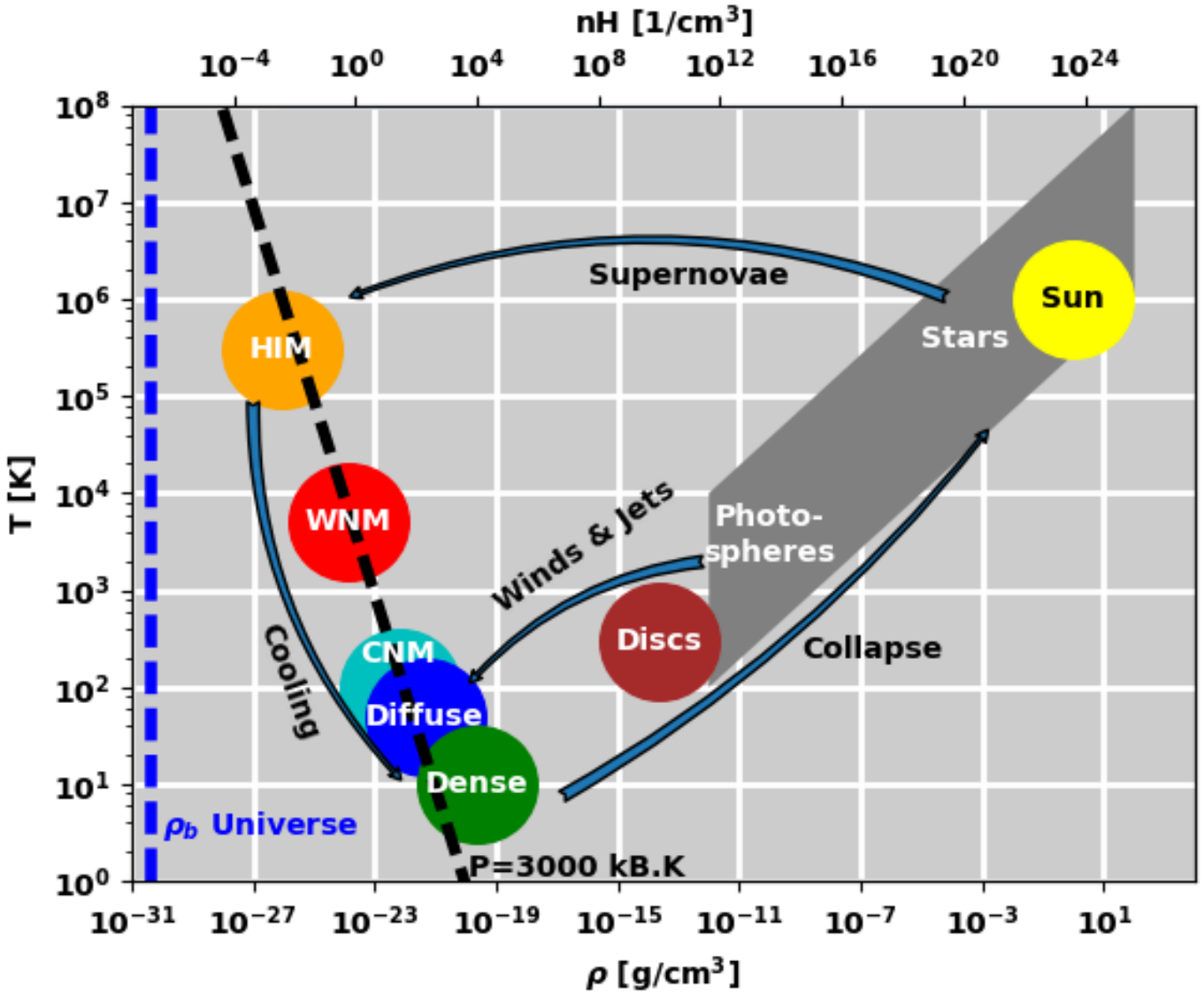

courtesy of P. Lesaffre

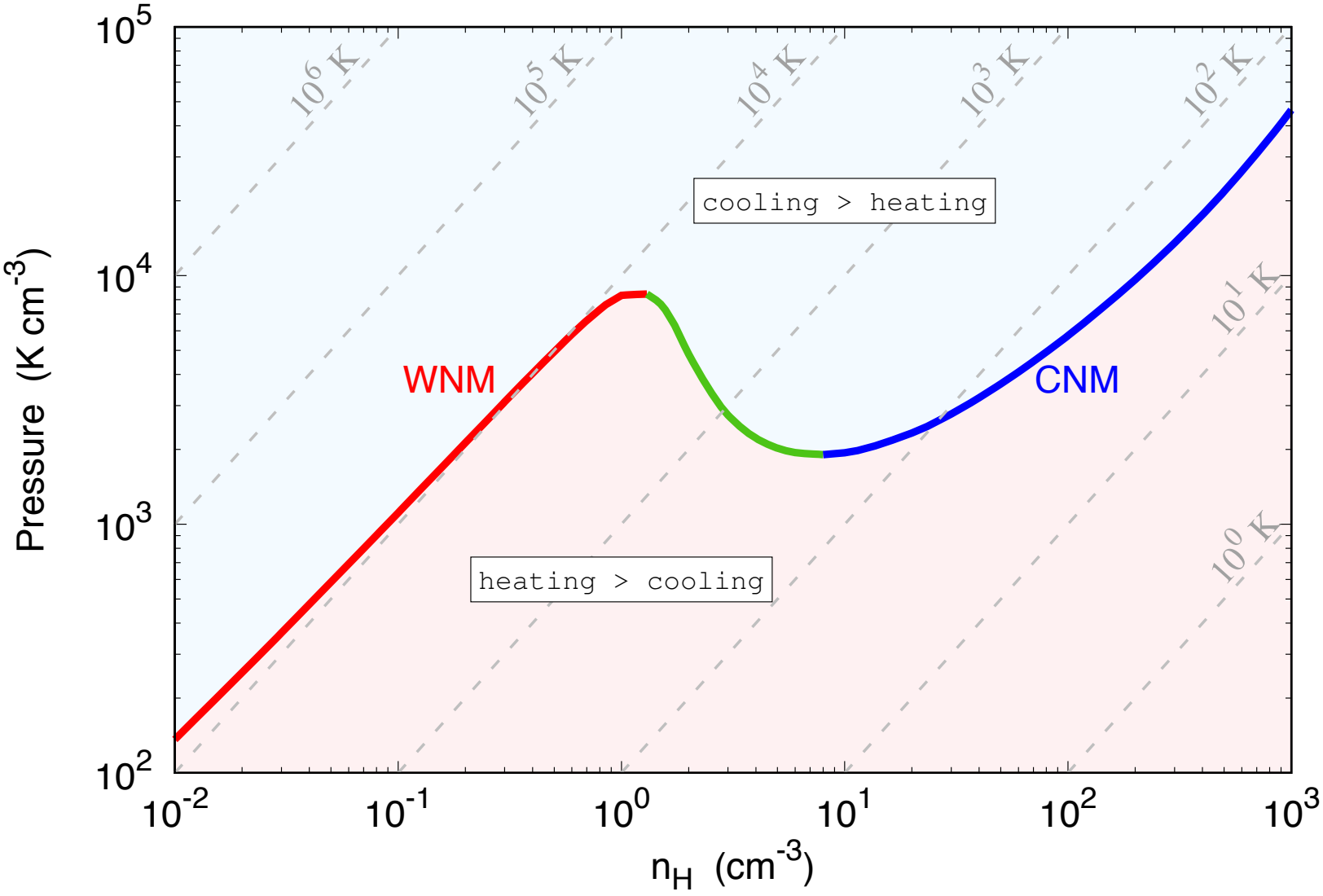
10^6 K
10^5 K
10^4 K
10^3 K
10^2 K
10^1 K
10^0 K
cooling > heating
heating > cooling
WNM
CNM
Pressure (K cm^{-3})
10^5
10^4
10^3
10^2
10^{-2}
10^{-1}
10^0
10^1
10^2
10^3
n_H (cm^{-3})

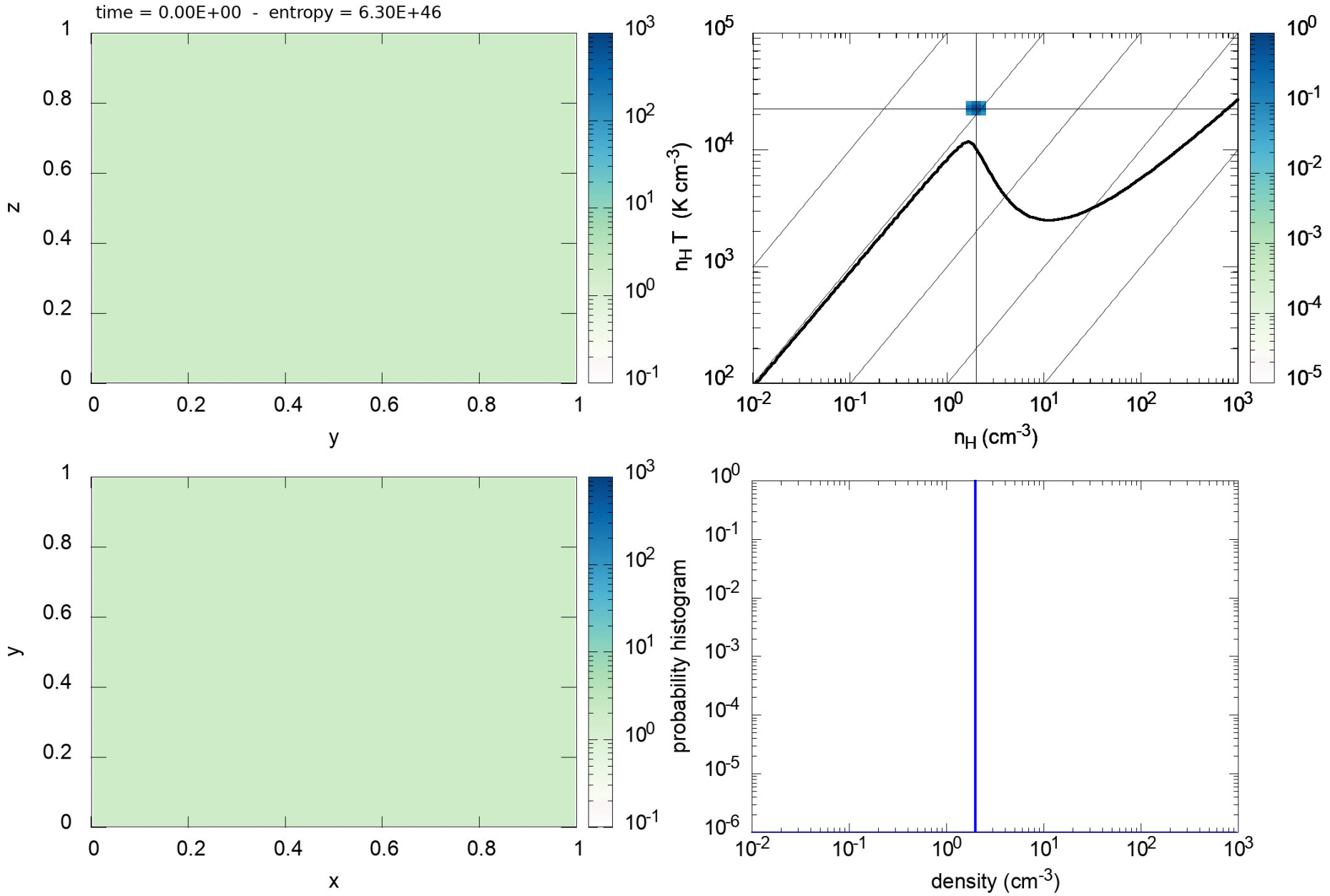
time = 0.00E+00 - entropy = 6.30E+46
z
y
x
n_H T (K cm^{-3})
n_H (cm^{-3})
probability histogram
density (cm^{-3})

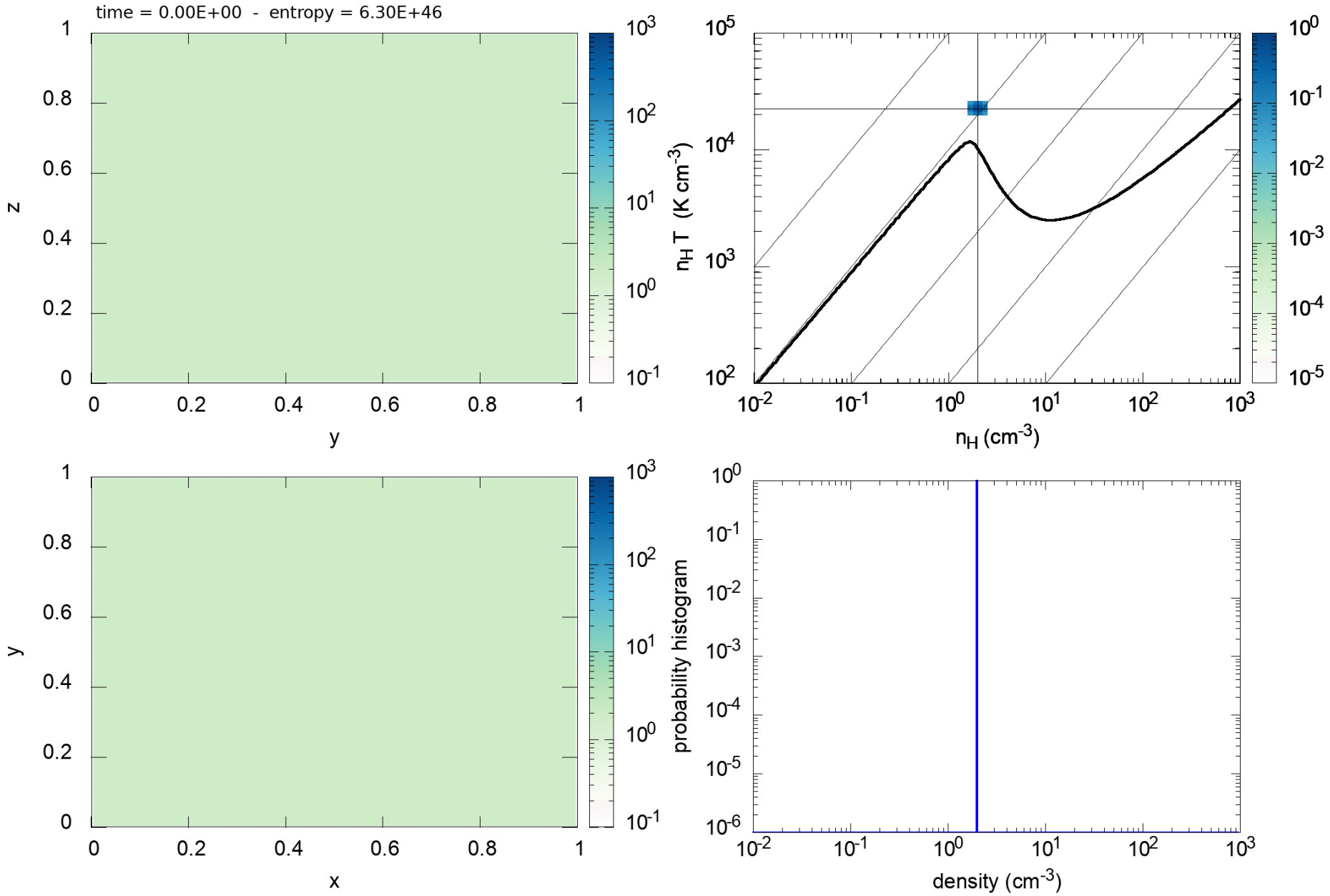
time = 0.00E+00 - entropy = 6.30E+46
z
y
n_H T (K cm^{-3})
n_H (cm^{-3})
y
x
probability histogram
density (cm^{-3})

probabilistic evolution

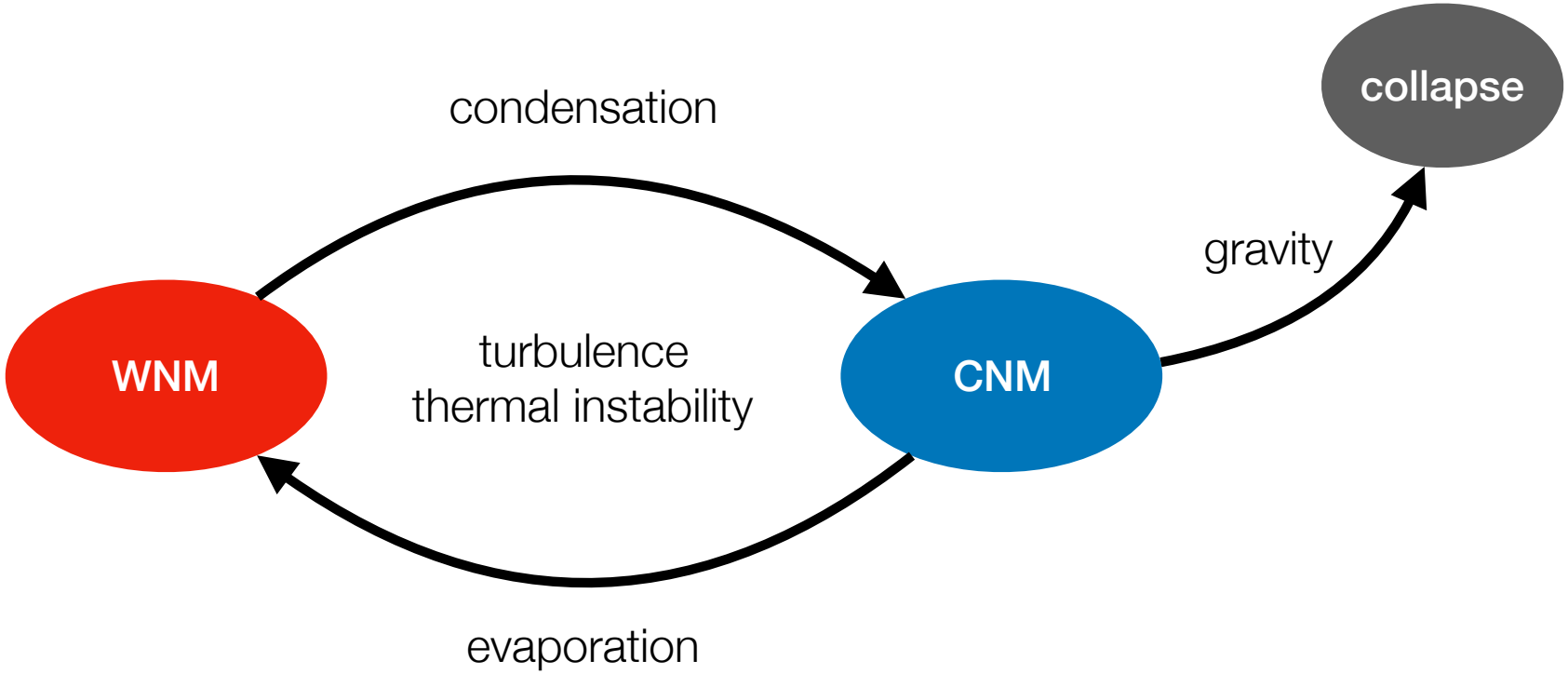

- distribution of phases ?
- rate of mass transfer ?
- transfer / dissipation of mechanical energy ?

chemical correlations

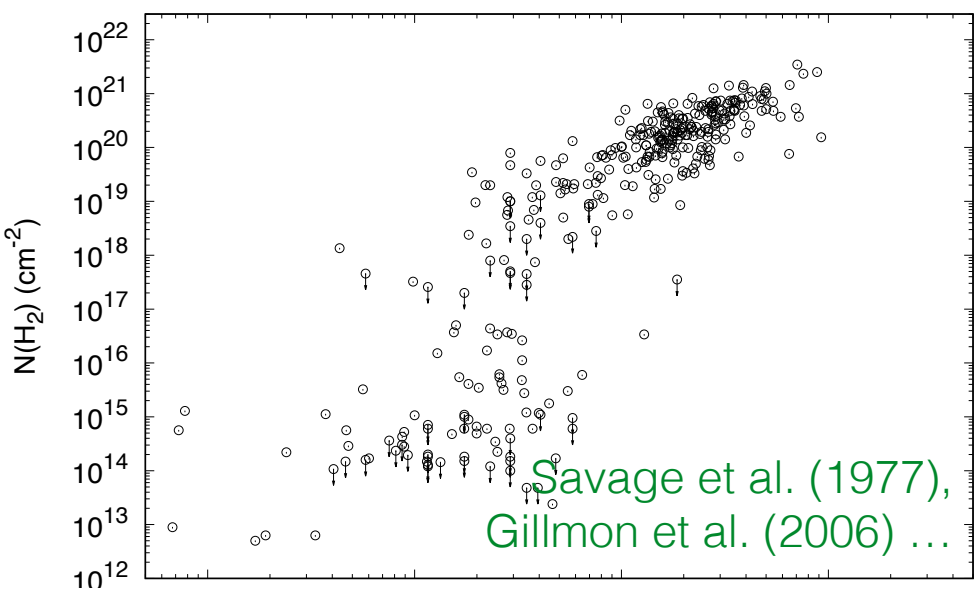

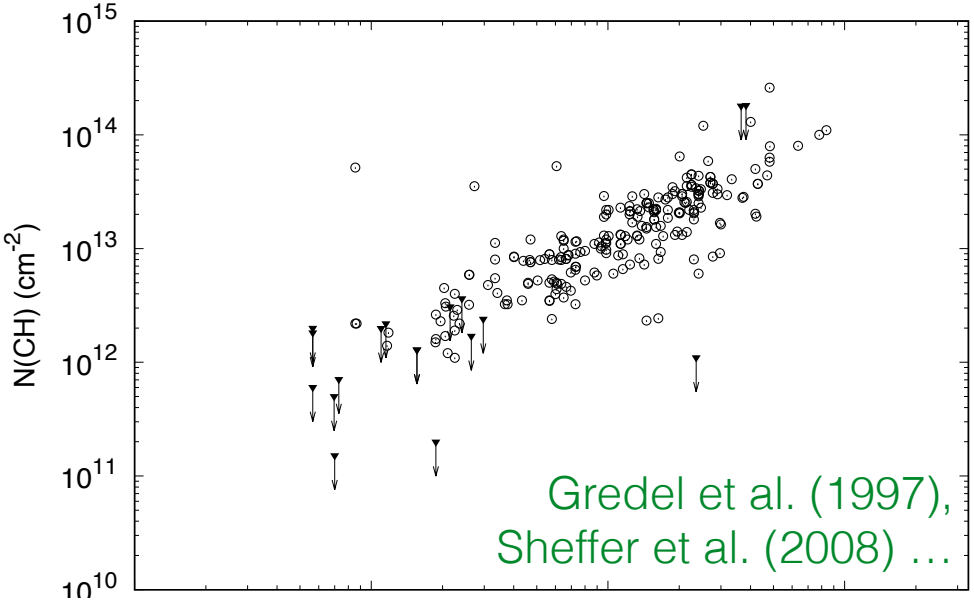

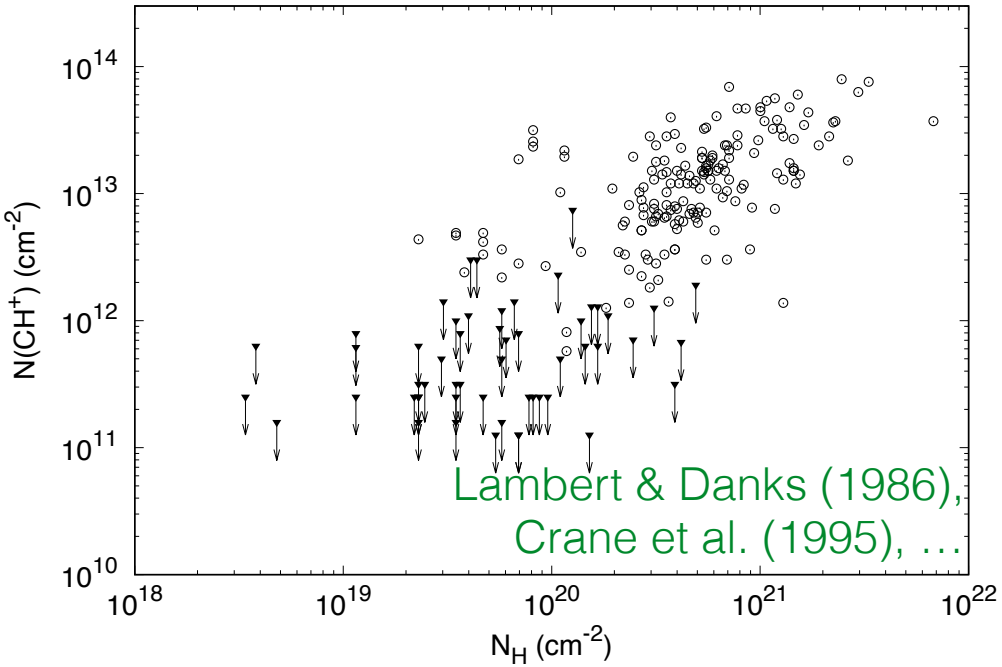

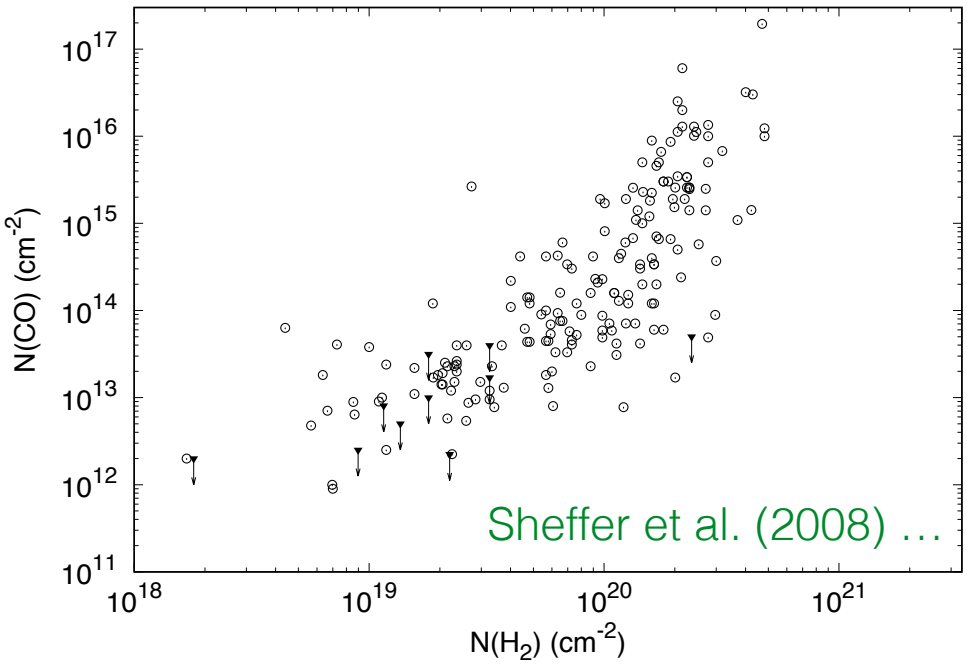

kinematics of molecules

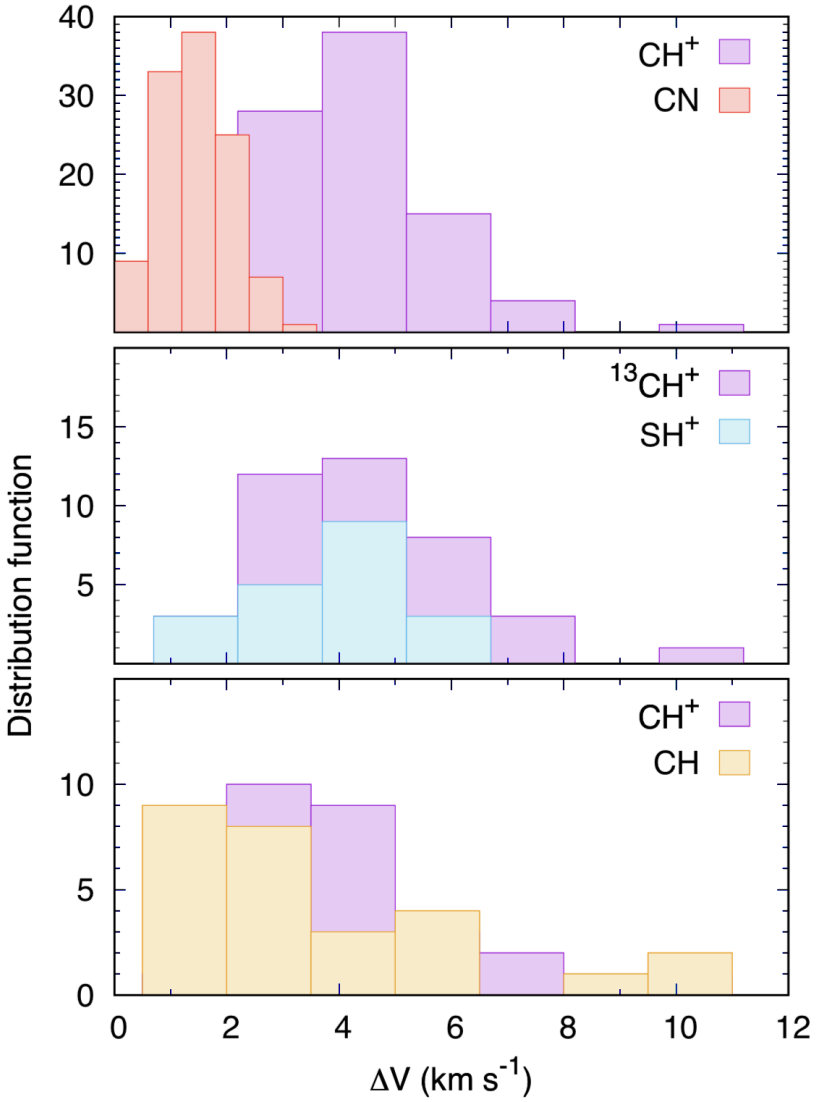

Crane et al. (1995)
Godard et al. (2012)

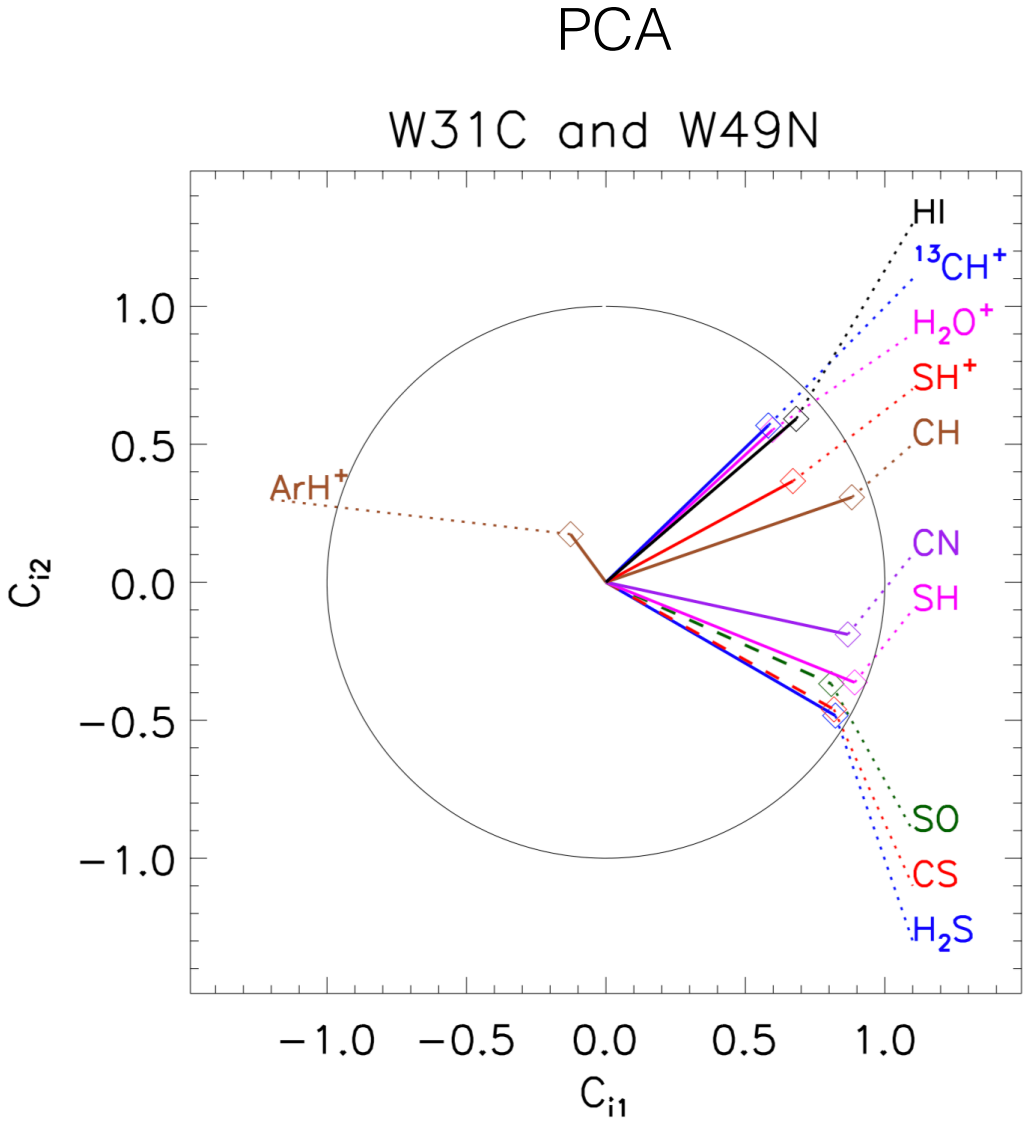

Neufeld et al. (2015)

1D static or steady-state models (Cloudy, Meudon PDR, Kosma-tau, PD-Shock, TDR, …)

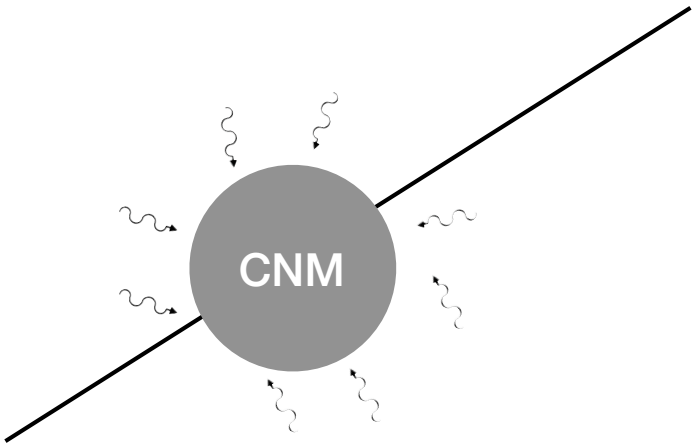

strengths

- detailed microphysical processes
- out-of-equilibrium processes
- solutions to MHD equations

interpretations

- local physical conditions
- observations → plausible distribution
- correlations limited to CNM

  CH^+ → dissipation in CNM

  H_2^* → dissipation in CNM

- no information on line profiles

1D static or steady-state models (Cloudy, Meudon PDR, Kosma-tau, PD-Shock, TDR, …)

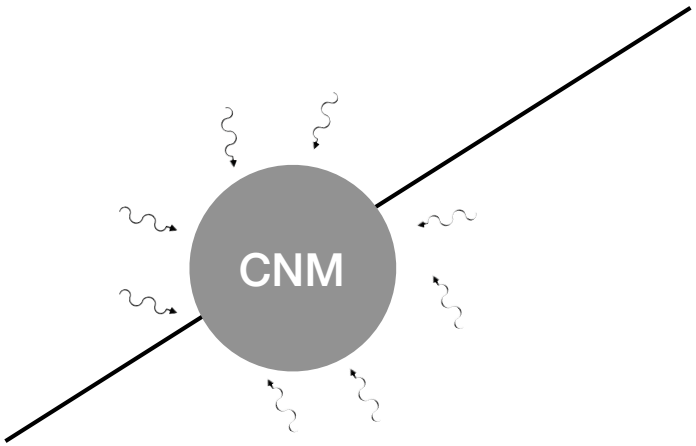

strengths

- detailed microphysical processes
- out-of-equilibrium processes
- solutions to MHD equations

interpretations

- global physical conditions
- observations ← probable distribution
- correlations ~~limited to CNM~~
  - CH^+ → ~~dissipation in CNM~~
  - H_2^* → ~~dissipation in CNM~~
- ~~no~~ information on line profiles

simulations of multiphase gas

RAMSES code (Teyssier 2002)

- periodic box size L
- mean density $\overline{n_H}$
- isotropic UV field G_0
- spectral forcing at ~ L / 2
- homogeneous B_x

↓

- 3D ideal MHD
- self-gravity
- heating / cooling
- evolution of H^+, H, and H_2

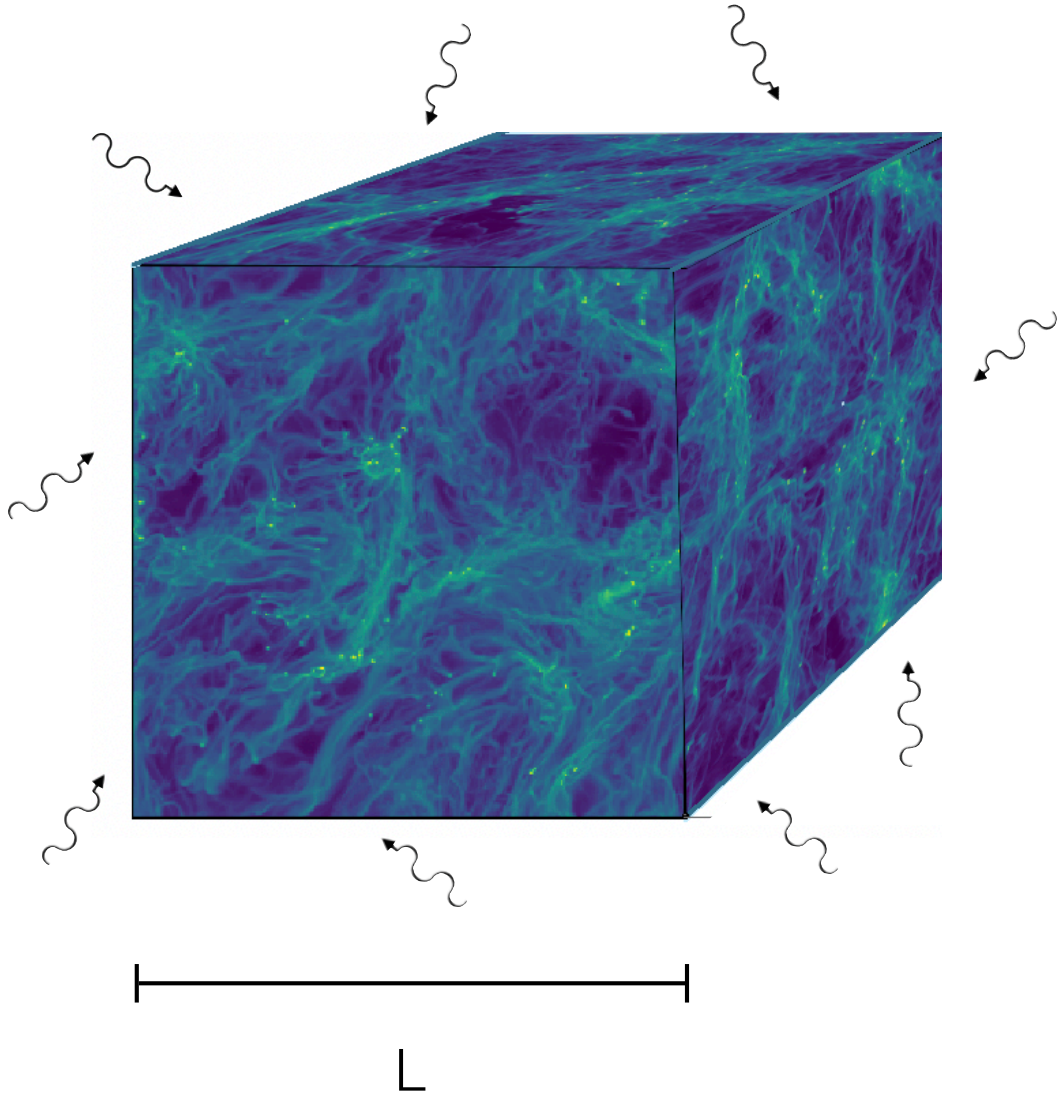

post-processing tools

chemical solver (Valdivia et al. 2017)

- 149 species (Le Petit et al. 2006)
- ~ 2000 reactions
- at equilibrium except H^+, H, H_2

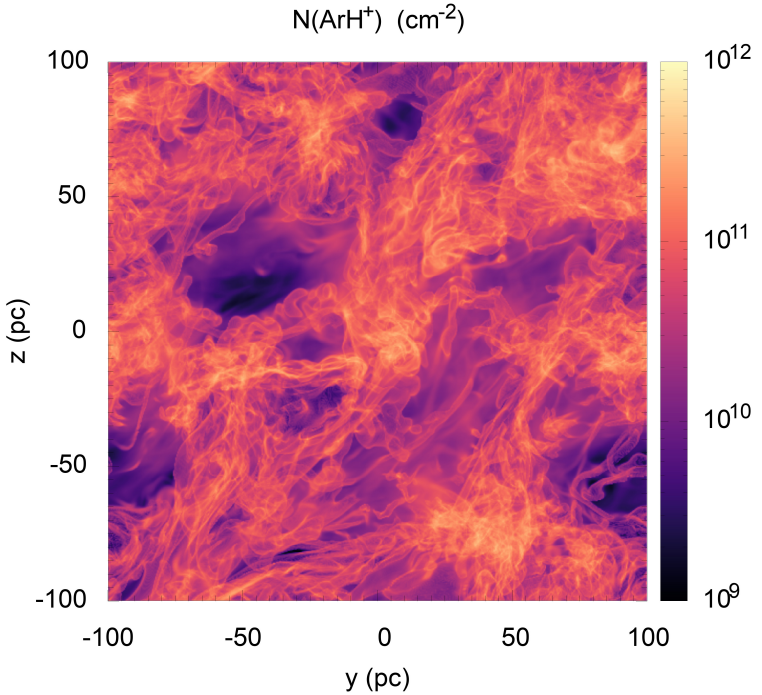

radiative transfer

- any lines (rot, vib, elec)
- excitation processes

non reactive collisions

radiative pumping (self-shield)

chemical reactions

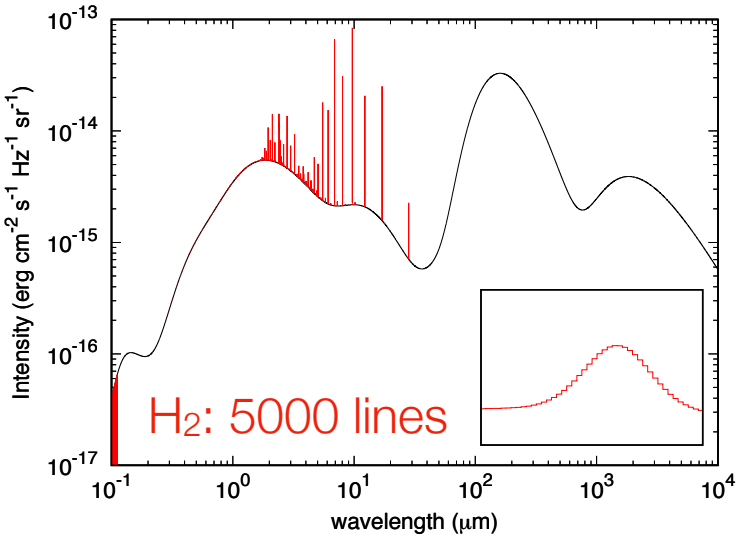

observational sample

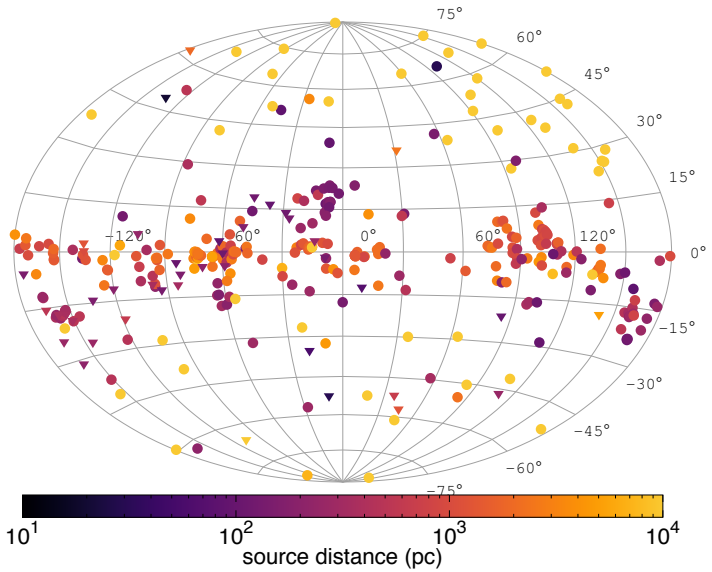

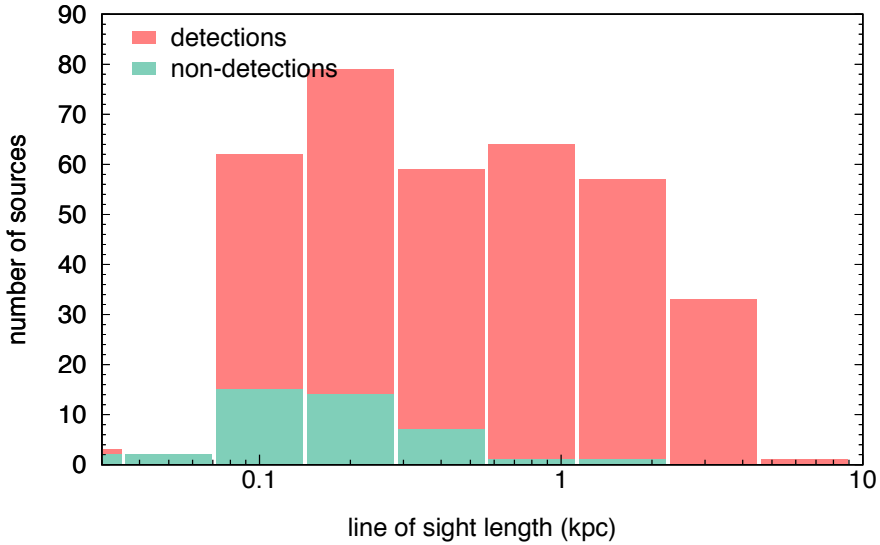

simulated sample

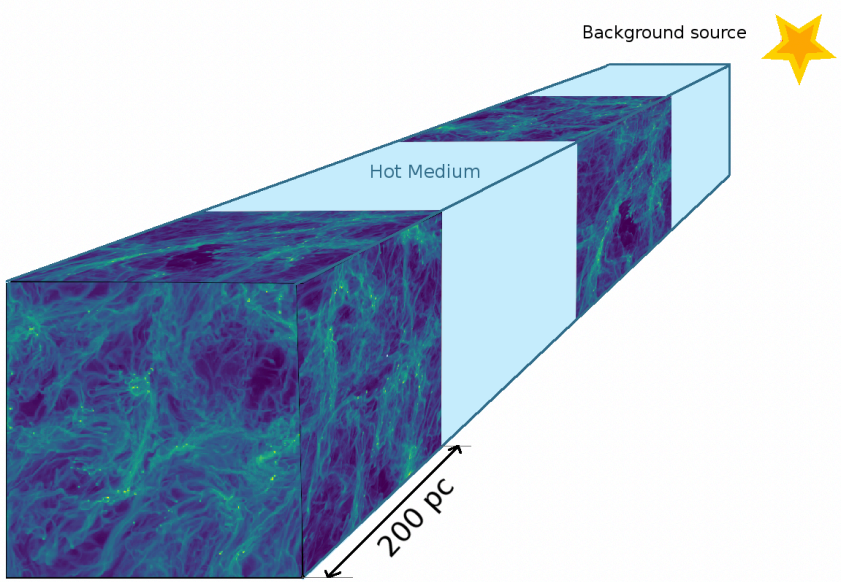

→ same length distribution

→ free parameter $\phi = 0.5$

grids of numerical simulations

- used : ~ 600
- published : ~ 100
- comp. time : 2 744 318 hours

cluster Totoro

ERC MIST (E. Falgarone)

exploration of parameters

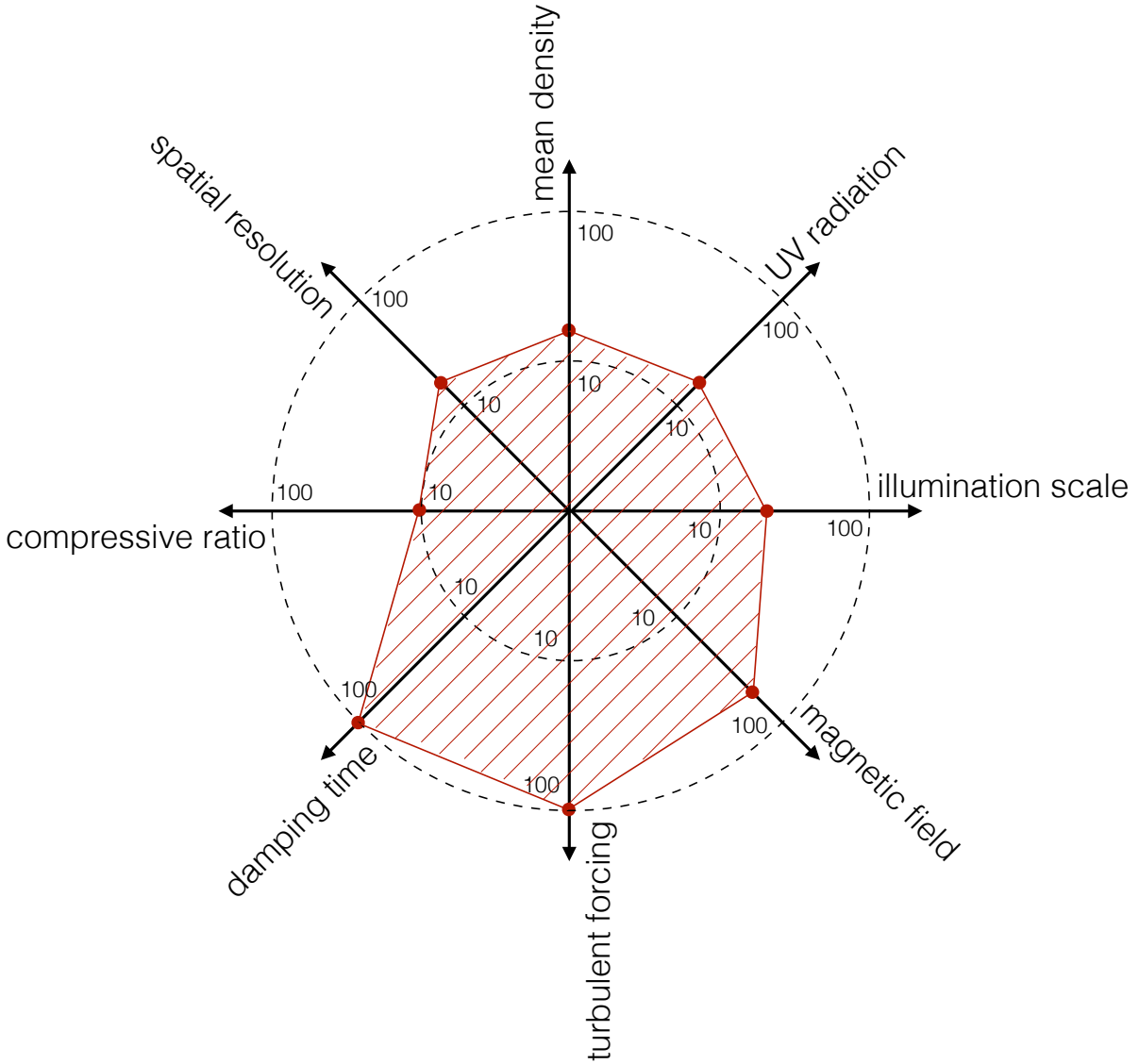

fiducial setup

parameters			
L	=	200	pc
$\overline{n_H}$	=	1.5	cm^{-3}
G_0	=	1	
F	=	$1.5\ 10^{-3}$	kpc Myr^{-2}
B_x	=	4	μG
R	=	512^3	

energetic properties			
<kin>	=	$1.7\ 10^{-12}$	erg cm^{-3}
<mag>	=	$1.6\ 10^{-12}$	erg cm^{-3}
<ther>	=	$1.0\ 10^{-12}$	erg cm^{-3}
<rad>	=	$1.6\ 10^{-12}$	erg cm^{-3}
$<\sigma_v>_{tur}$	=	5.4	km s^{-1}

phase & thermal pressure distributions

$$f_{\rm WNM} = 35\% \quad f_{\rm LNM} = 11\% \quad f_{\rm CNM} = 54\%$$

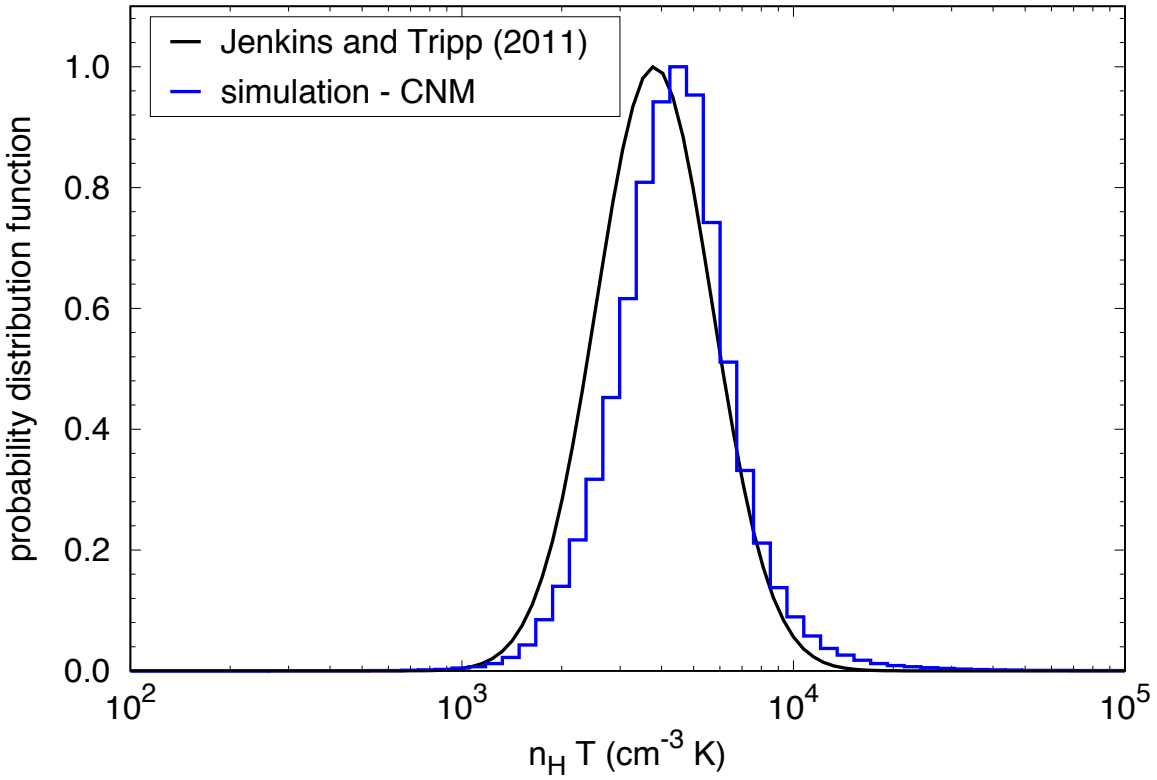

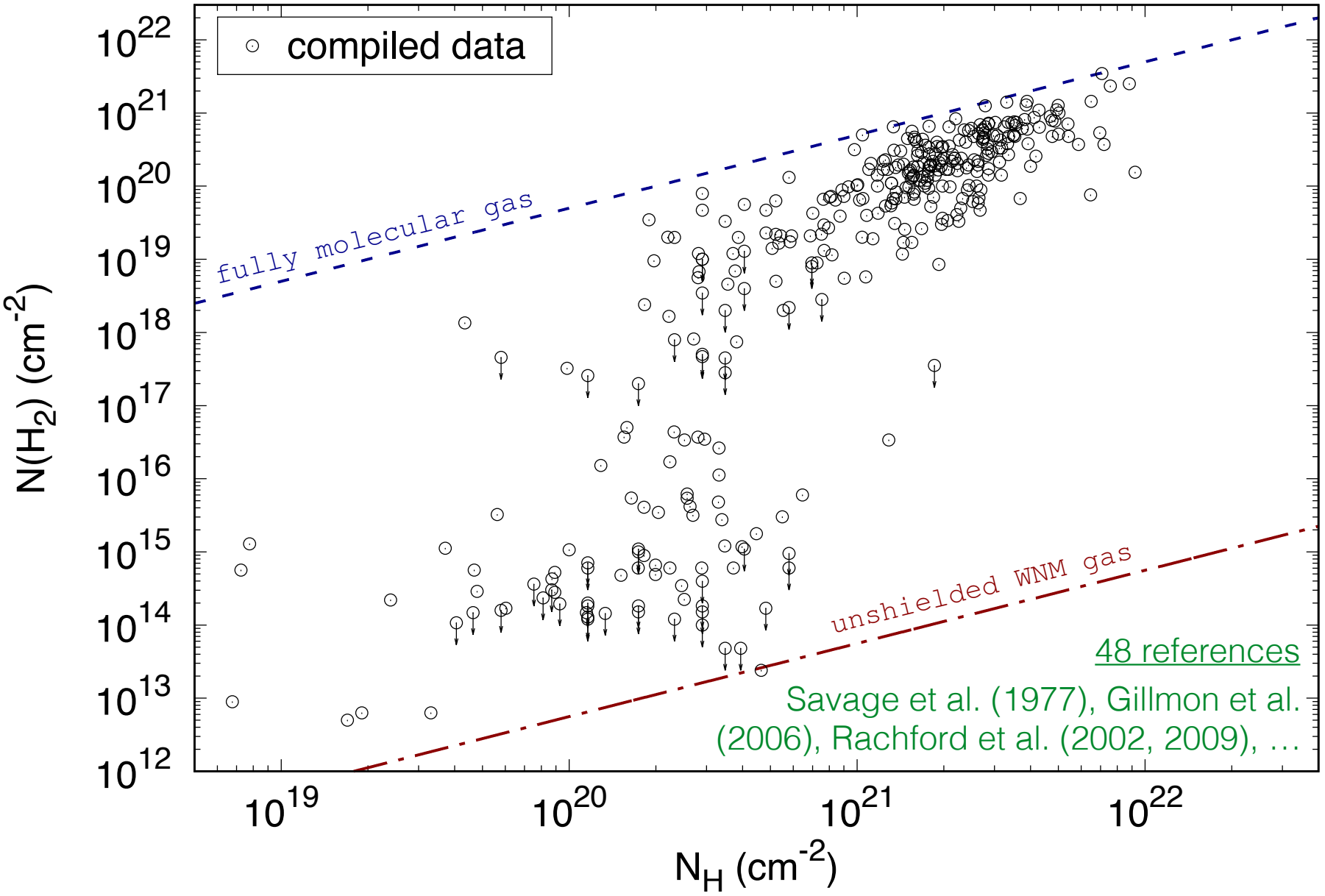
compiled data
fully molecular gas
unshielded WNM gas
48 references
Savage et al. (1977), Gillmon et al. (2006), Rachford et al. (2002, 2009), …
$N(H_2)$ (cm^{-2})
N_H (cm^{-2})
10^{12}
10^{13}
10^{14}
10^{15}
10^{16}
10^{17}
10^{18}
10^{19}
10^{20}
10^{21}
10^{22}

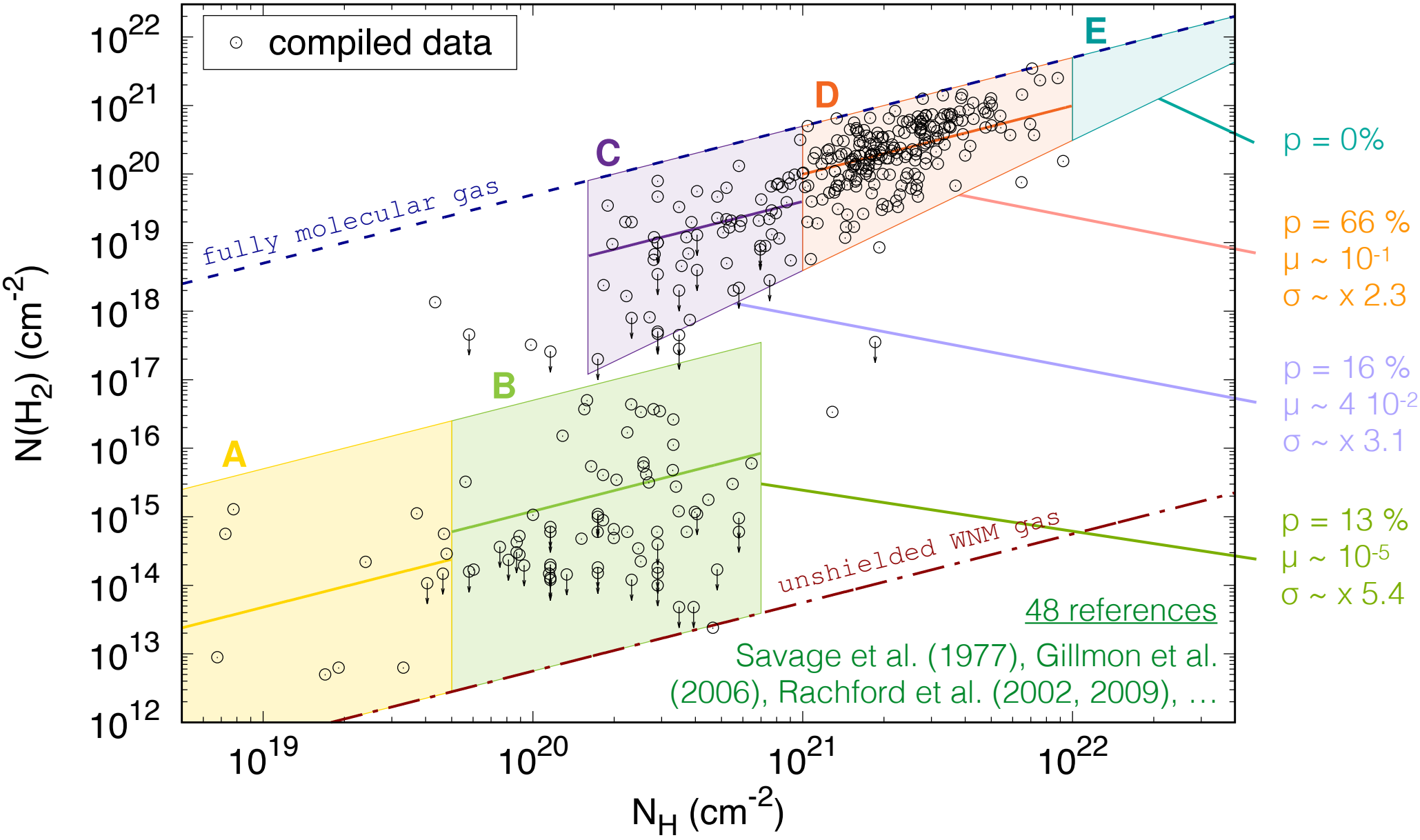
compiled data
fully molecular gas
unshielded WNM gas
A
B
C
D
E
p = 0%
p = 66 %
μ ~ 10-1
σ ~ x 2.3
p = 16 %
μ ~ 4 10-2
σ ~ x 3.1
p = 13 %
μ ~ 10-5
σ ~ x 5.4
48 references
Savage et al. (1977), Gillmon et al. (2006), Rachford et al. (2002, 2009), …
N(H2) (cm-2)
NH (cm-2)
10^22
10^21
10^20
10^19
10^18
10^17
10^16
10^15
10^14
10^13
10^12
10^19
10^20
10^21
10^22

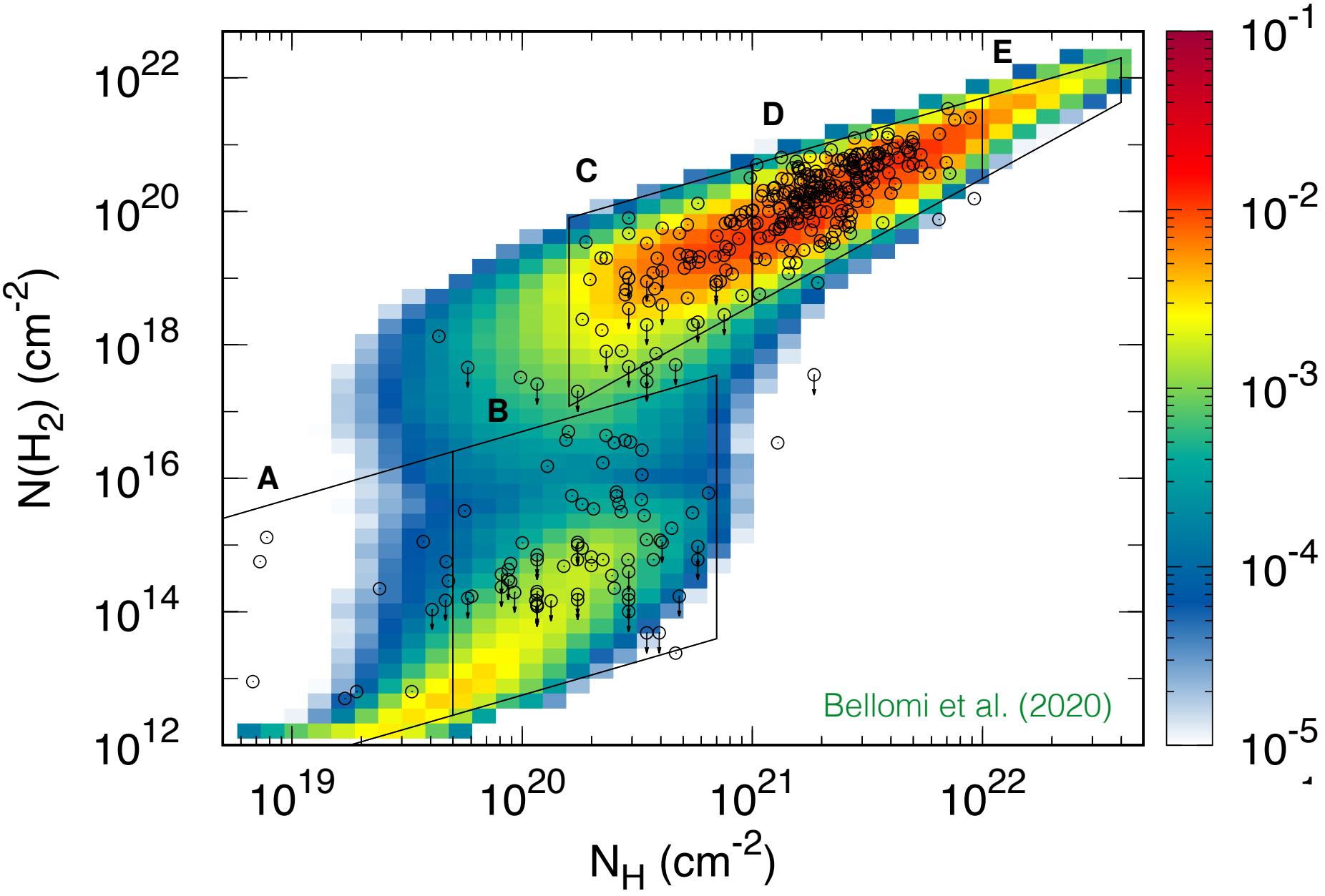
A
B
C
D
E
Bellomi et al. (2020)
$N(H_2)$ (cm^{-2})
N_H (cm^{-2})
10^{22}
10^{20}
10^{18}
10^{16}
10^{14}
10^{12}
10^{19}
10^{20}
10^{21}
10^{22}
10^{-1}
10^{-2}
10^{-3}
10^{-4}
10^{-5}

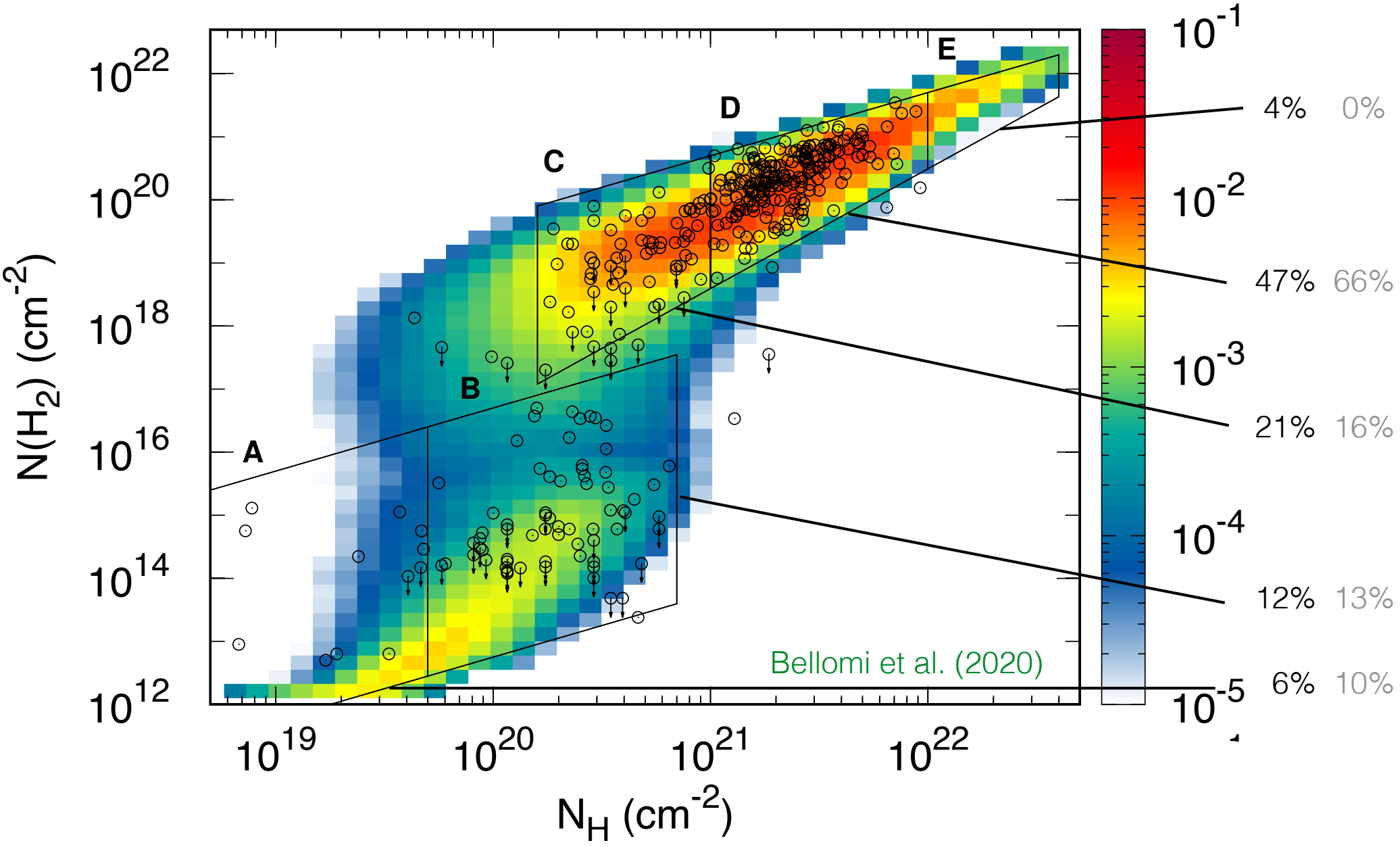
A
B
C
D
E
4% 0%
47% 66%
21% 16%
12% 13%
6% 10%
Bellomi et al. (2020)
$N(H_2)$ (cm^{-2})
N_H (cm^{-2})
10^{22}
10^{20}
10^{18}
10^{16}
10^{14}
10^{12}
10^{19}
10^{20}
10^{21}
10^{22}
10^{-1}
10^{-2}
10^{-3}
10^{-4}
10^{-5}

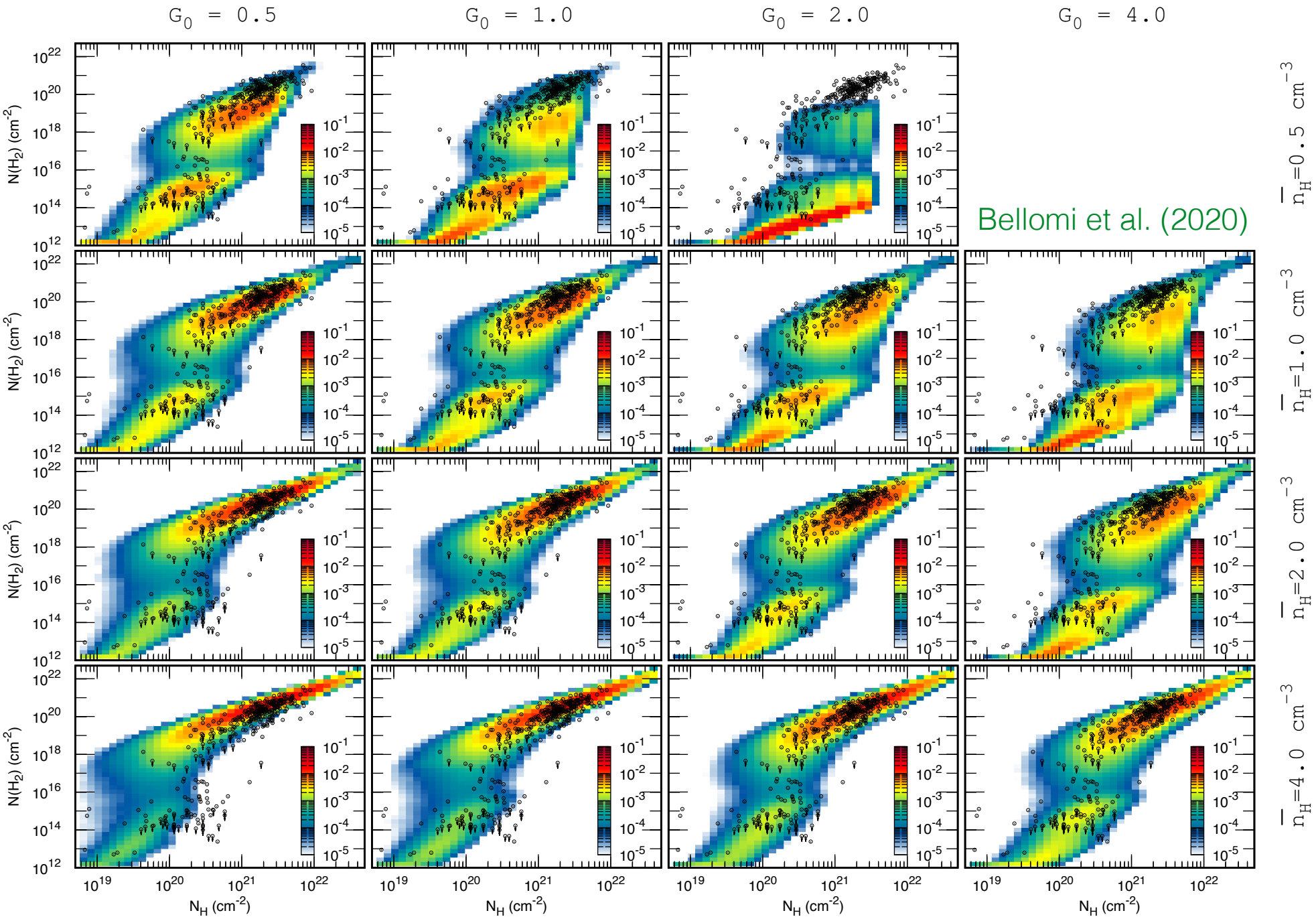

Bellomi et al. (2020)

The CH^+ conundrum

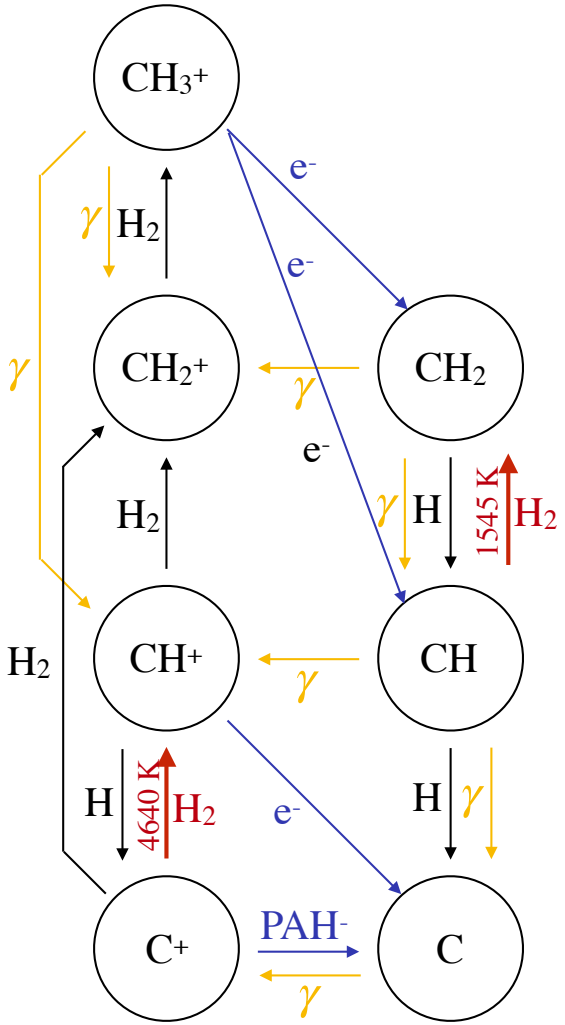

Neufeld et al. (2015)

only efficient formation pathway

$C^+ + H_2 \longrightarrow CH^+ + H$ $\quad \Delta E/k \sim 4640$ K

need warm environments

need H_2 mainly formed in CNM

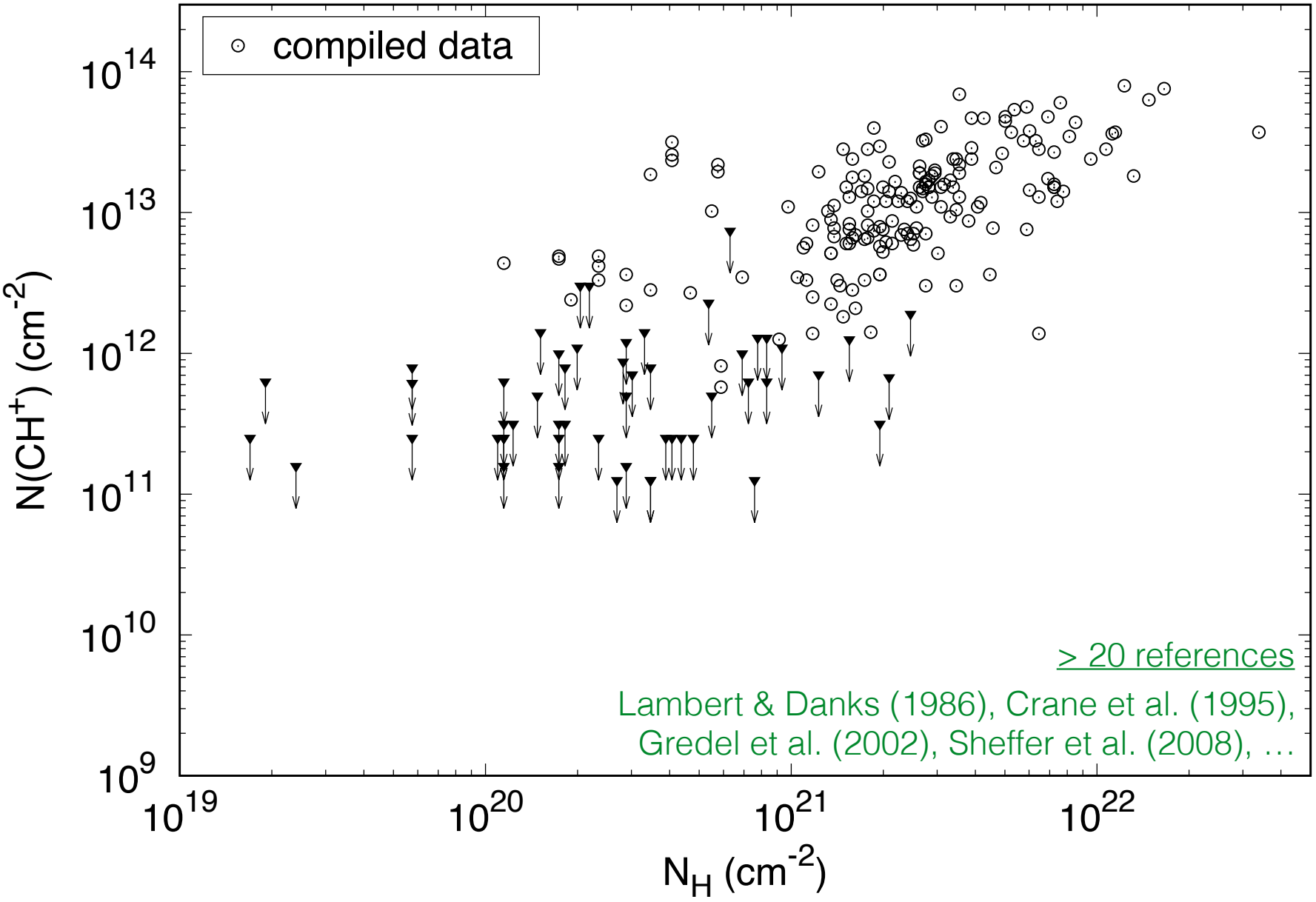
compiled data
10^{14}
10^{13}
10^{12}
10^{11}
10^{10}
10^{9}
$N(CH^+)$ (cm^{-2})
10^{19}
10^{20}
10^{21}
10^{22}
N_H (cm^{-2})
> 20 references
Lambert & Danks (1986), Crane et al. (1995),
Gredel et al. (2002), Sheffer et al. (2008), …

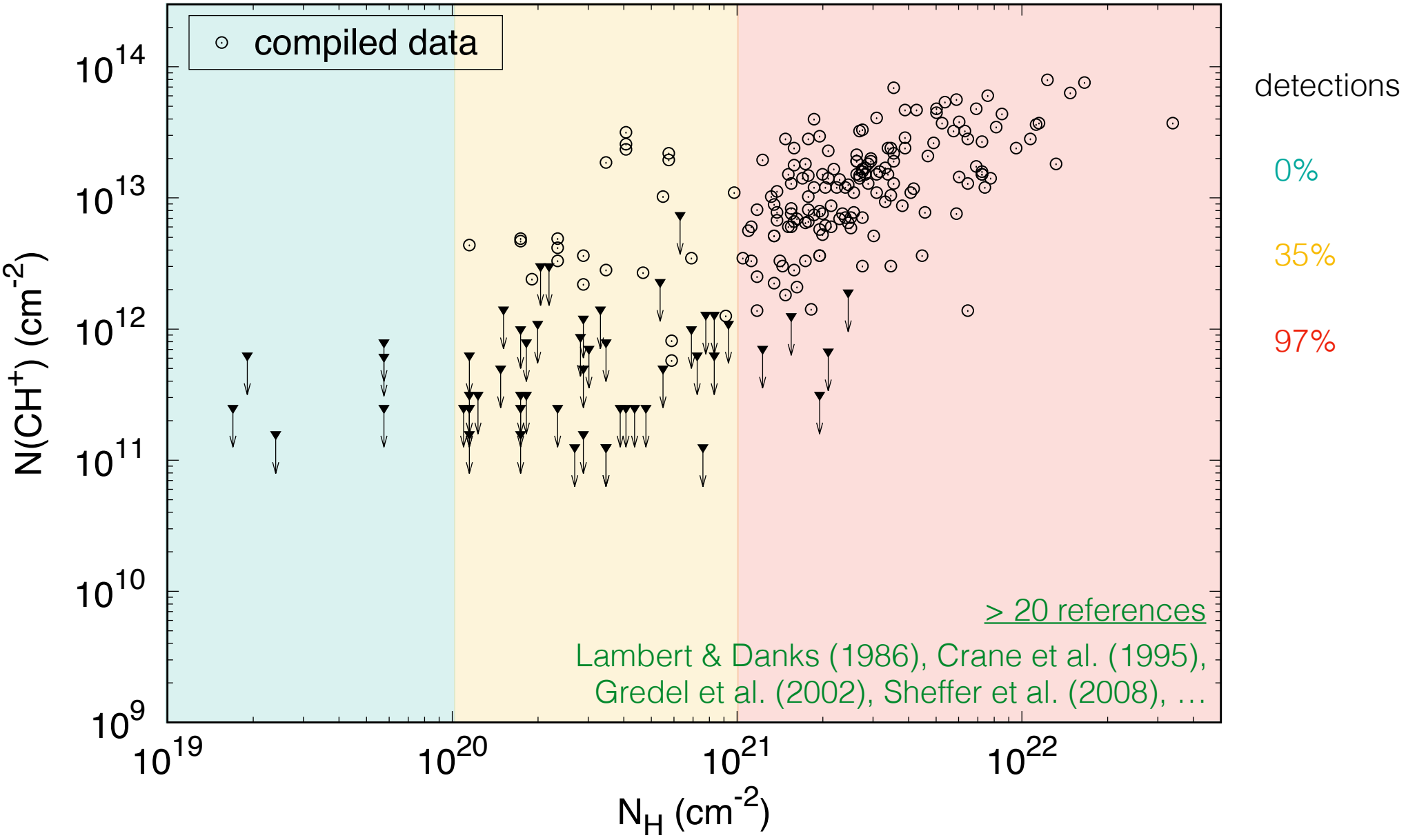
compiled data
10^{14}
10^{13}
10^{12}
10^{11}
10^{10}
10^{9}
$N(CH^+)$ (cm^{-2})
10^{19}
10^{20}
10^{21}
10^{22}
N_H (cm^{-2})
detections
0%
35%
97%
> 20 references
Lambert & Danks (1986), Crane et al. (1995),
Gredel et al. (2002), Sheffer et al. (2008), …

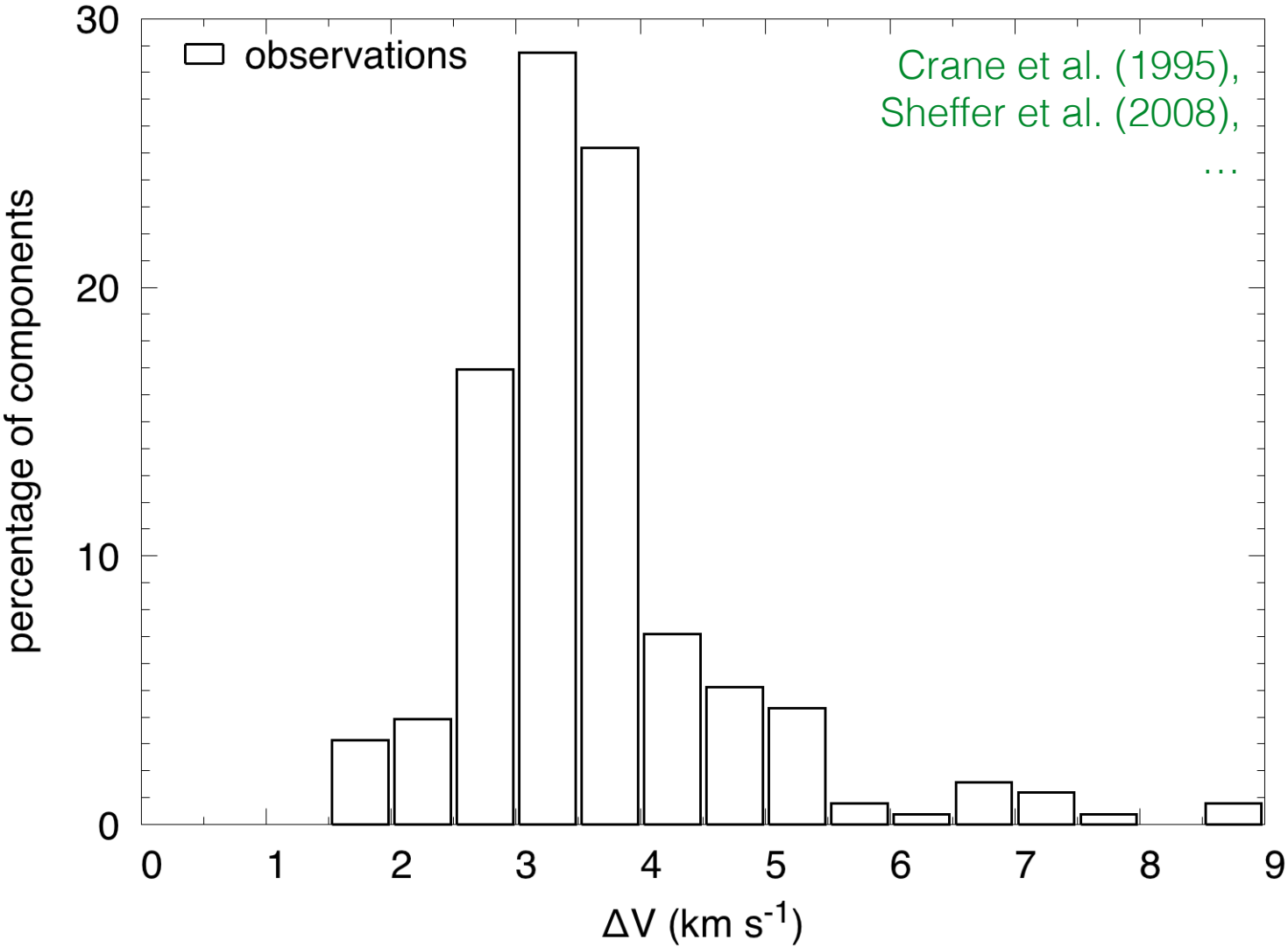

120 lines of sight

254 velocity components

$\Delta V \sim 3.59 \pm 1.18$ km s^{-1}

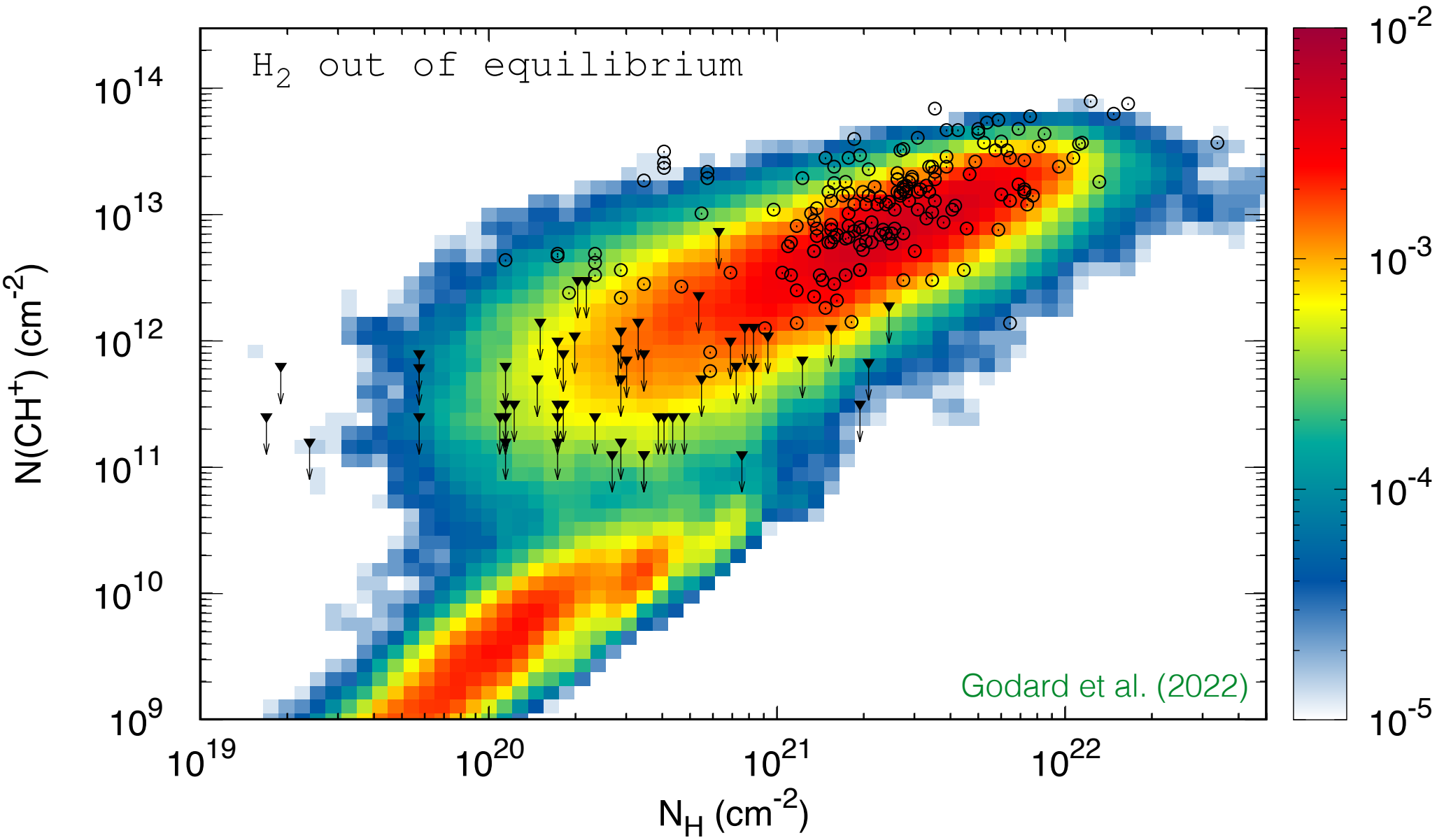
H2 out of equilibrium
Godard et al. (2022)
N(CH+) (cm-2)
NH (cm-2)
10^14
10^13
10^12
10^11
10^10
10^9
10^19
10^20
10^21
10^22
10^-2
10^-3
10^-4
10^-5

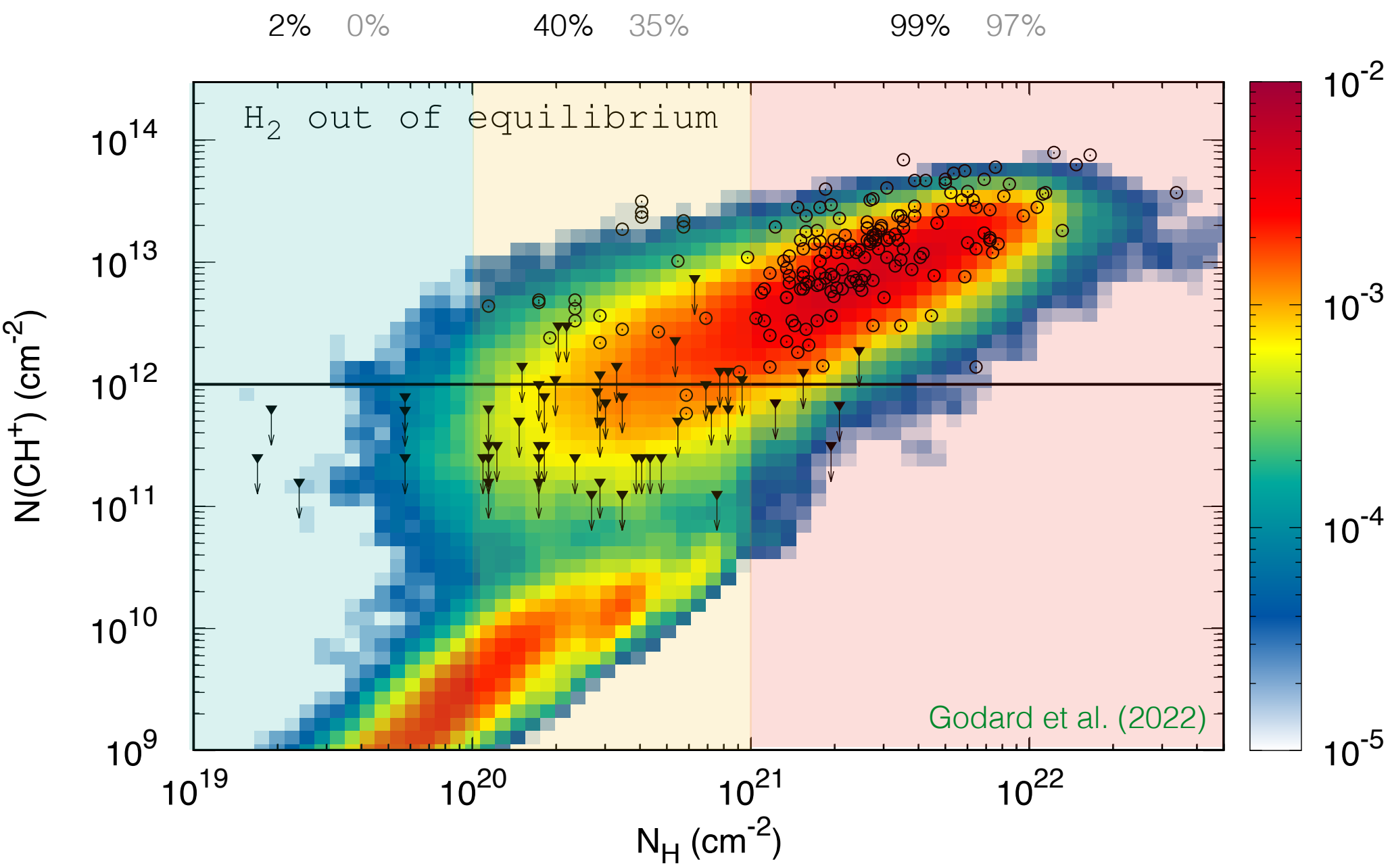
2%
0%
40%
35%
99%
97%
H_2 out of equilibrium
Godard et al. (2022)
$N(CH^+)$ (cm^{-2})
N_H (cm^{-2})
10^{14}
10^{13}
10^{12}
10^{11}
10^{10}
10^{9}
10^{19}
10^{20}
10^{21}
10^{22}
10^{-2}
10^{-3}
10^{-4}
10^{-5}

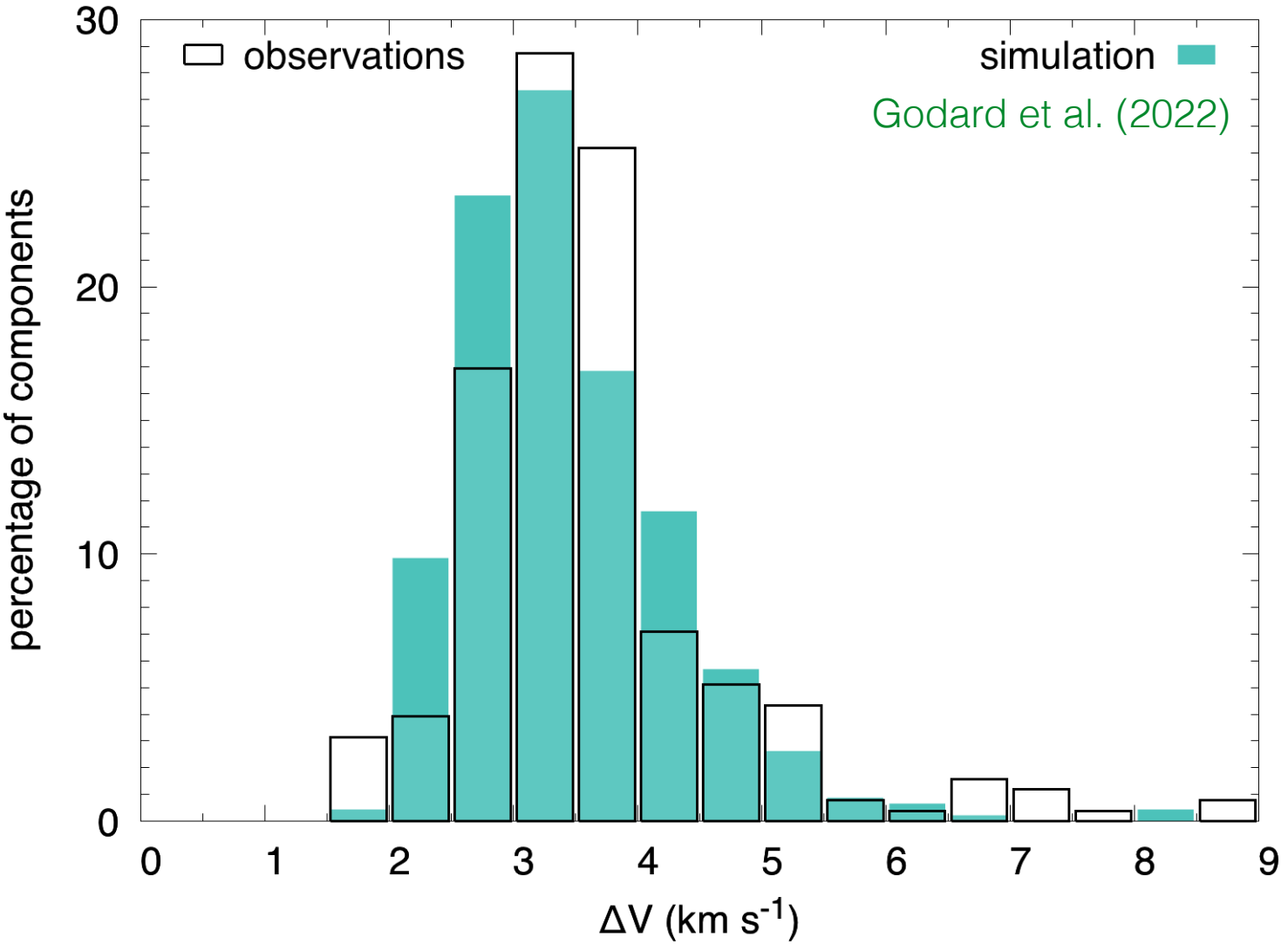

120 lines of sight

254 velocity components

$\Delta V \sim 3.59 \pm 1.18$ km s^{-1}

200 lines of sight

457 velocity components

$\Delta V \sim 3.44 \pm 0.87$ km s^{-1}

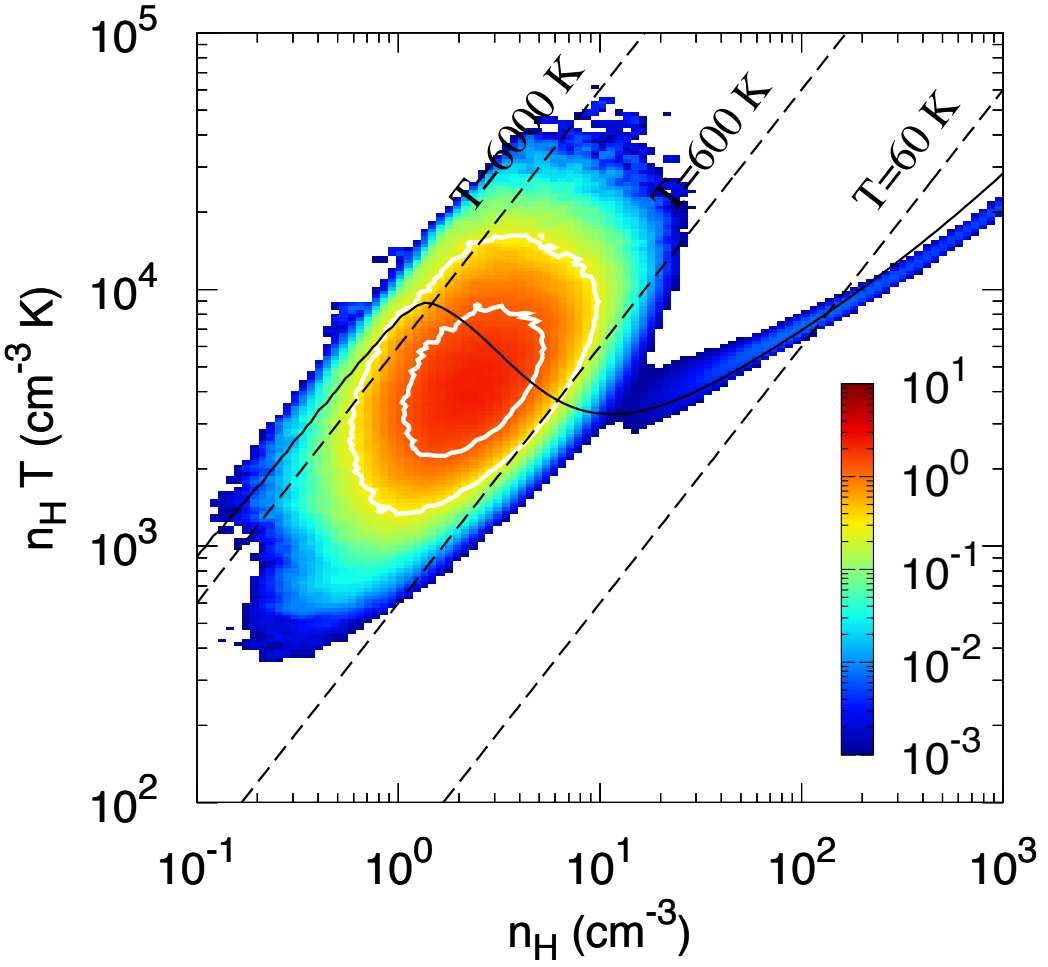

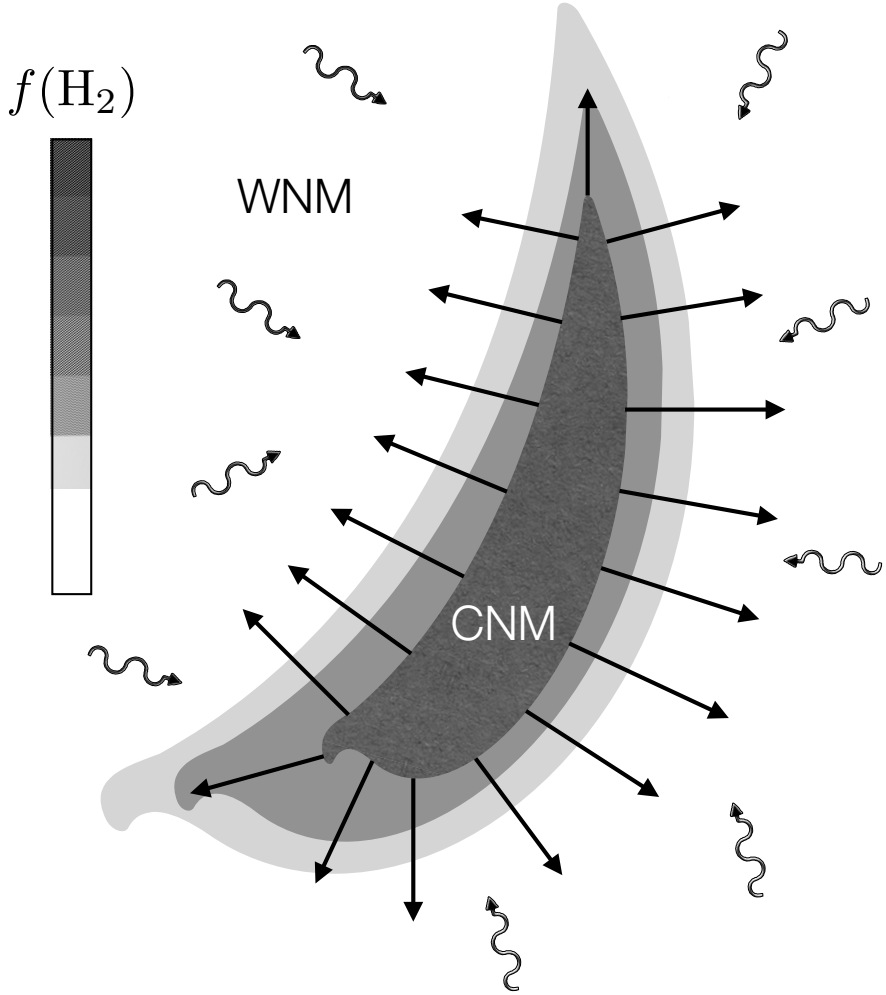

→ mass of CH+ from unstable gas rich in H_2

→ distribution depends on evaporation of CNM, i.e. mass transfer rate between phases

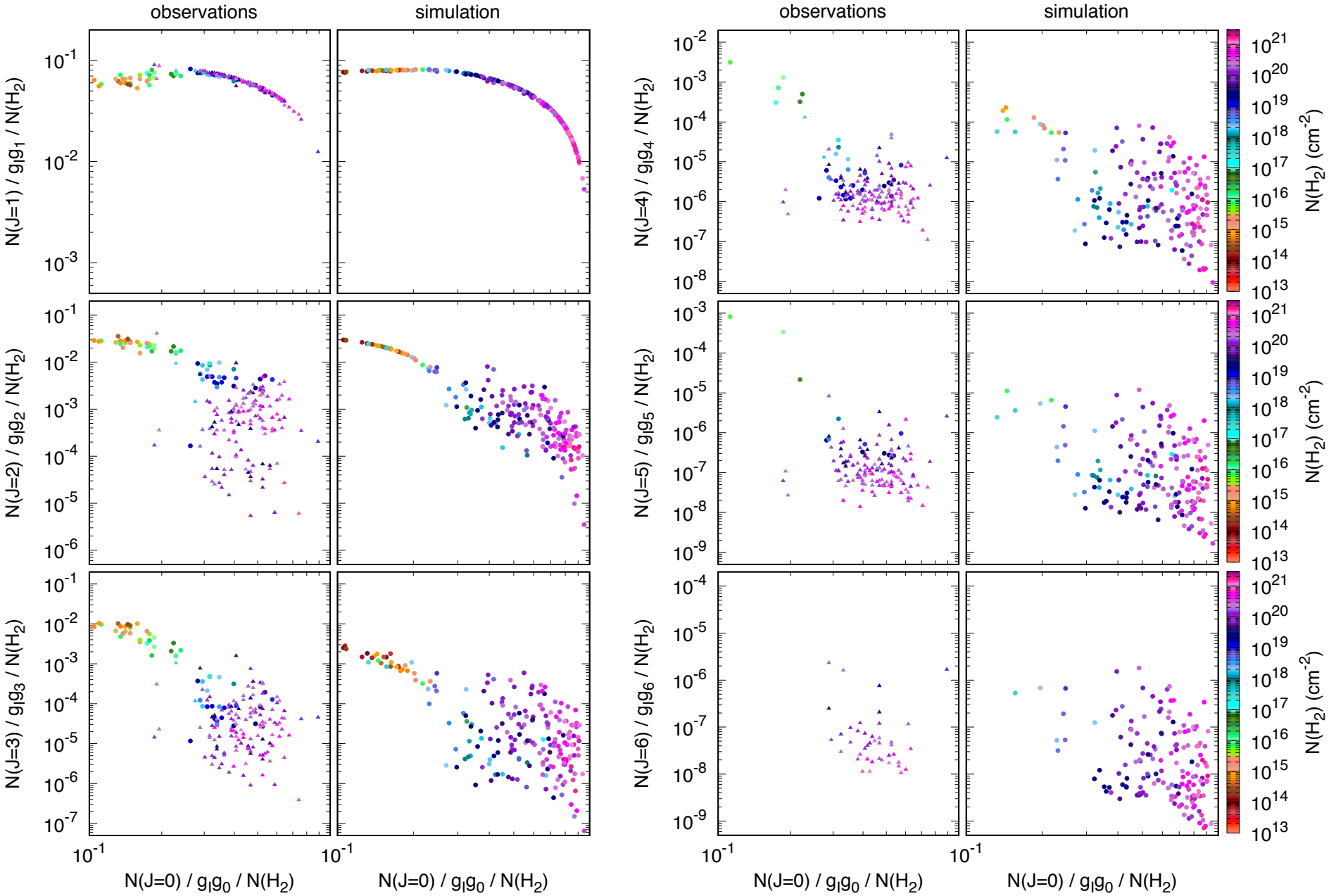
observations
simulation
observations
simulation
N(J=1) / g_l g_1 / N(H_2)
N(J=2) / g_l g_2 / N(H_2)
N(J=3) / g_l g_3 / N(H_2)
N(J=4) / g_l g_4 / N(H_2)
N(J=5) / g_l g_5 / N(H_2)
N(J=6) / g_l g_6 / N(H_2)
N(J=0) / g_l g_0 / N(H_2)
N(J=0) / g_l g_0 / N(H_2)
N(J=0) / g_l g_0 / N(H_2)
N(J=0) / g_l g_0 / N(H_2)
N(H_2) (cm^-2)
N(H_2) (cm^-2)

- Observational samples ⟶ global conditions

- A single simulation of turbulent multiphase ISM explains ~120 constraints
  - mass fractions & pressure distribution
  - statistics of H-to-H_2 transition
  - distribution of CH^+ & line profiles
  - distribution of excited H_2

- extension to other chemical tracer
  - N-d probability distributions
  - generalization of the KS-test
  - continuum emission
  - predictions for JWST & SKA
  - faraday rotation measures
  - magnetic field distribution

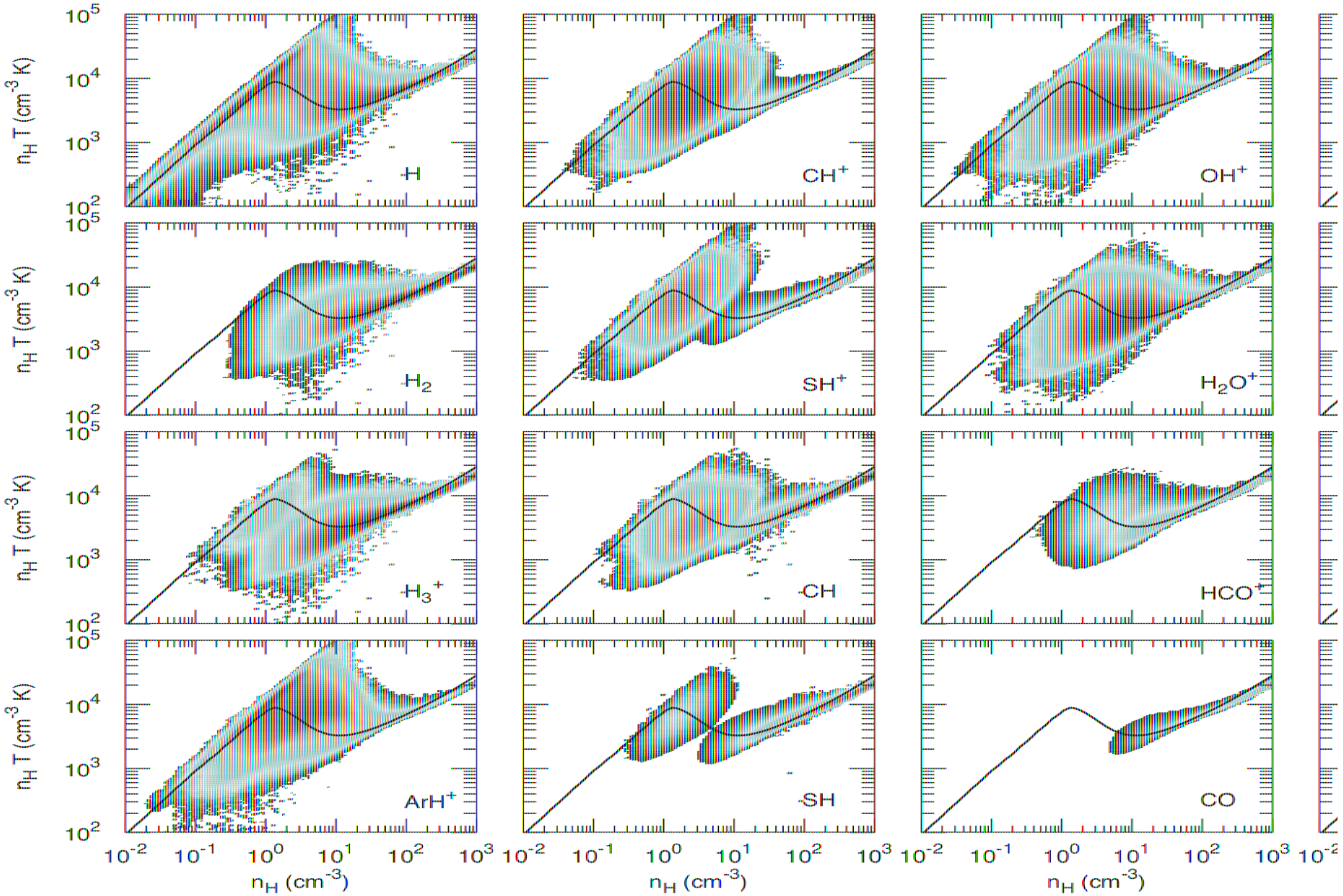
H
CH+
OH+
H2
SH+
H2O+
H3+
CH
HCO+
ArH+
SH
CO
nH T (cm-3 K)
nH (cm-3)
10^5
10^4
10^3
10^2
10^-2
10^-1
10^0
10^1
10^2
10^3

multiphase neutral ISM

Heiles and Troland (2003)
Murray et al. (2018)

WNM → n_H ~ 0.5 cm^{-3} T ~ 7000 K
50 %, mostly atomic

LNM → T ~ 300 K - 5000 K
20 %

CNM → n_H ~ 50 cm^{-3} T ~ 70 K
30 %, partly molecular

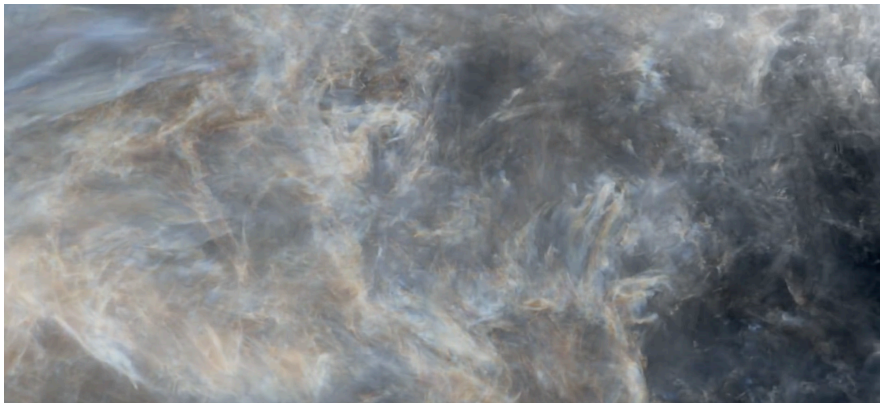

HI survey - Peek et al. (2018)

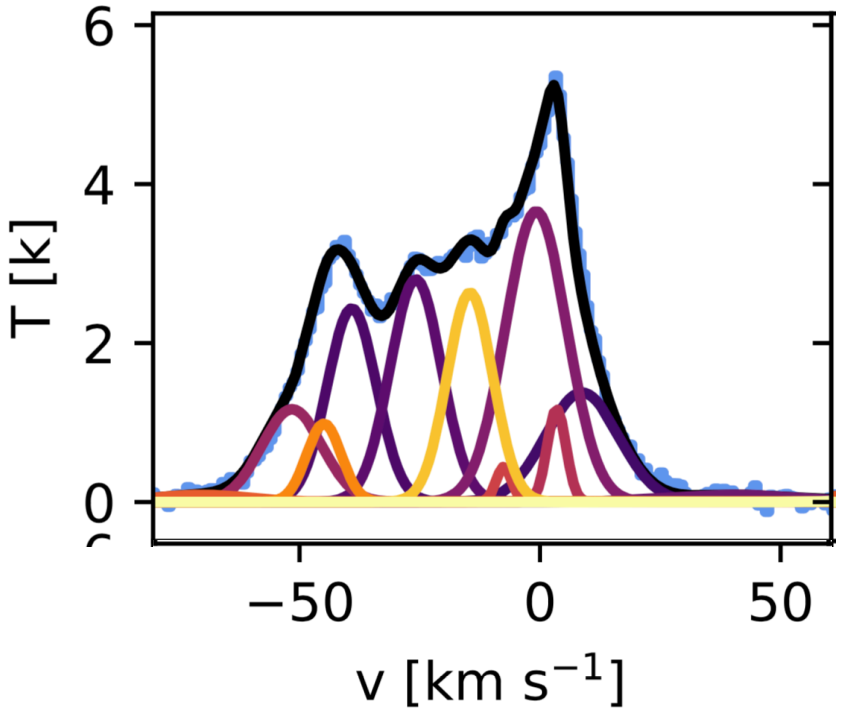

ROHSA - Marchal et al. (2019)

galactic structure

exponential decrease of

- density
- molecular fraction

with

- galactocentric distance R_{gal}
- height above the plane z

local properties

- $n_H \sim 1.5$ cm^{-3}
- $G_0 = 10^8$ ph cm^{-2} s^{-1}
- $f_{H2} = 10^{-1}$

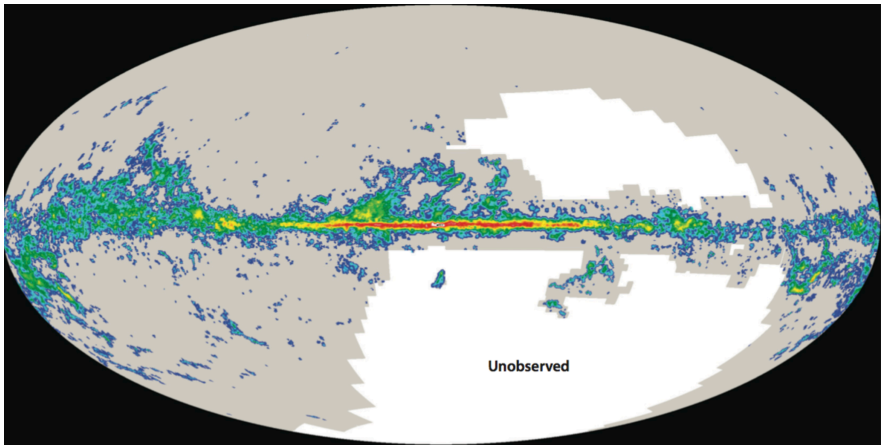

12CO survey - Dame et al. (2001)

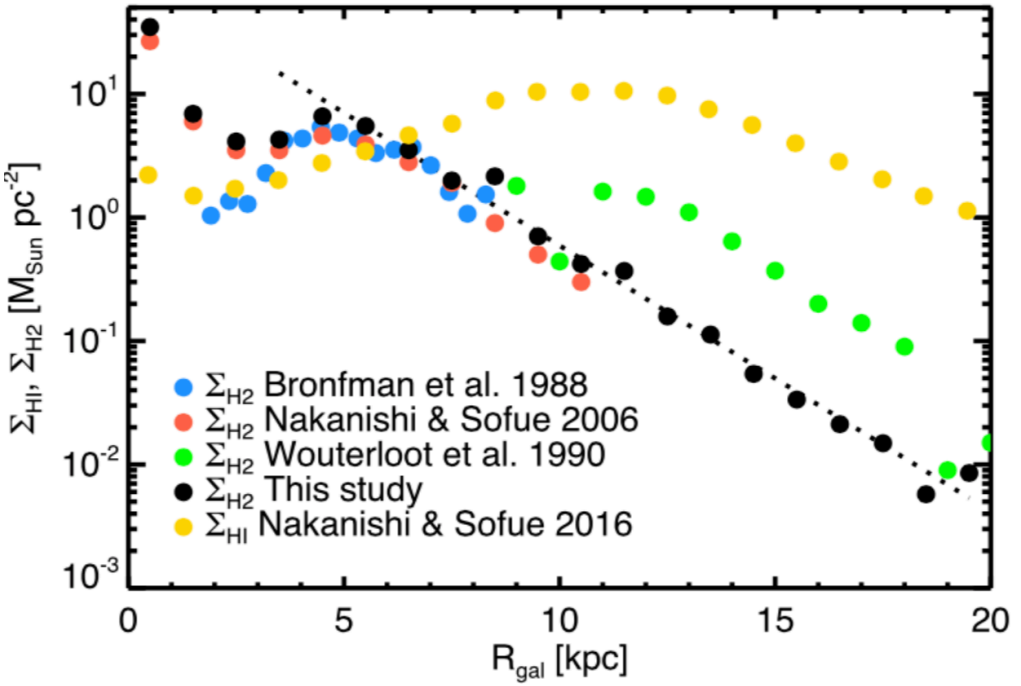

Miville-Deschênes et al. (2017)

numerical simulations of turbulent ISM

Hennebelle & Perault (1999)
Koyama & Inutsuka (2002)
Vazquez-Semadeni et al. (2003)
Hennebelle & Audit (2007)
Inoue & Inutsuka (2009)
Gazol & Kim (2010)
…

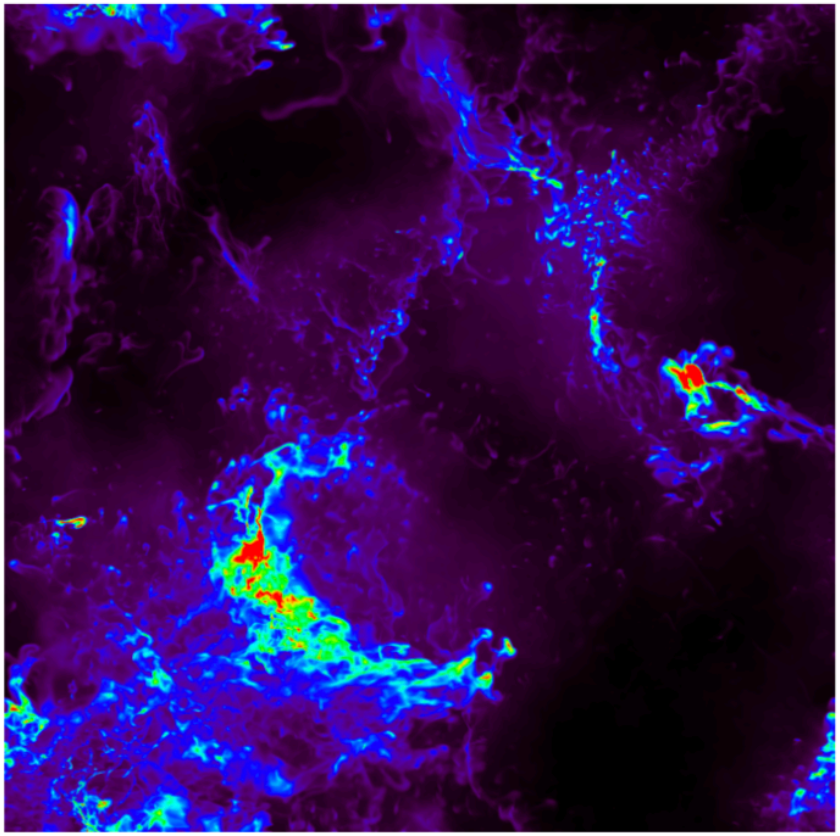

Saury et al. (2014)

mass fractions

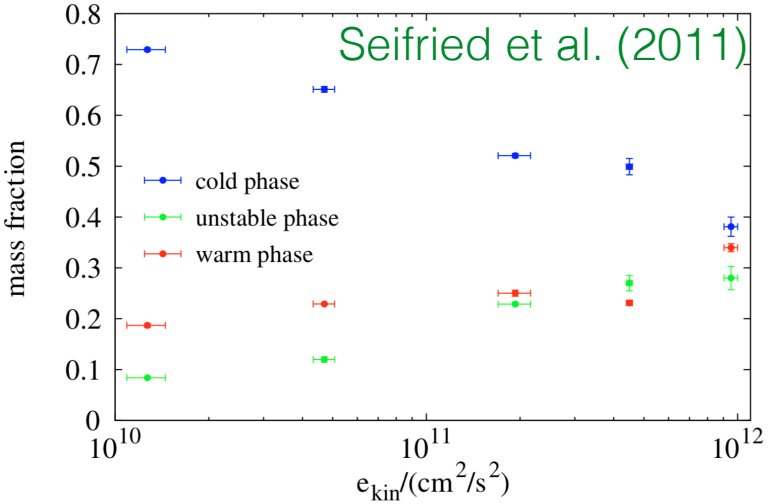

pressure distribution

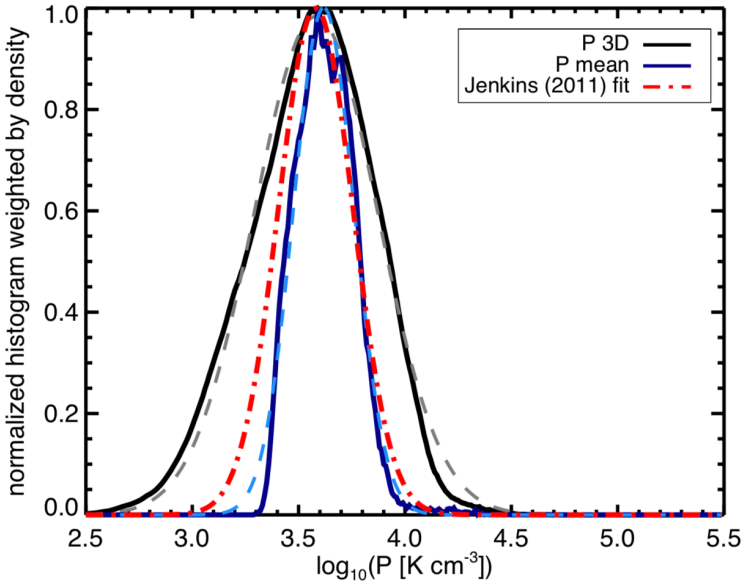

Saury et al. (2014)

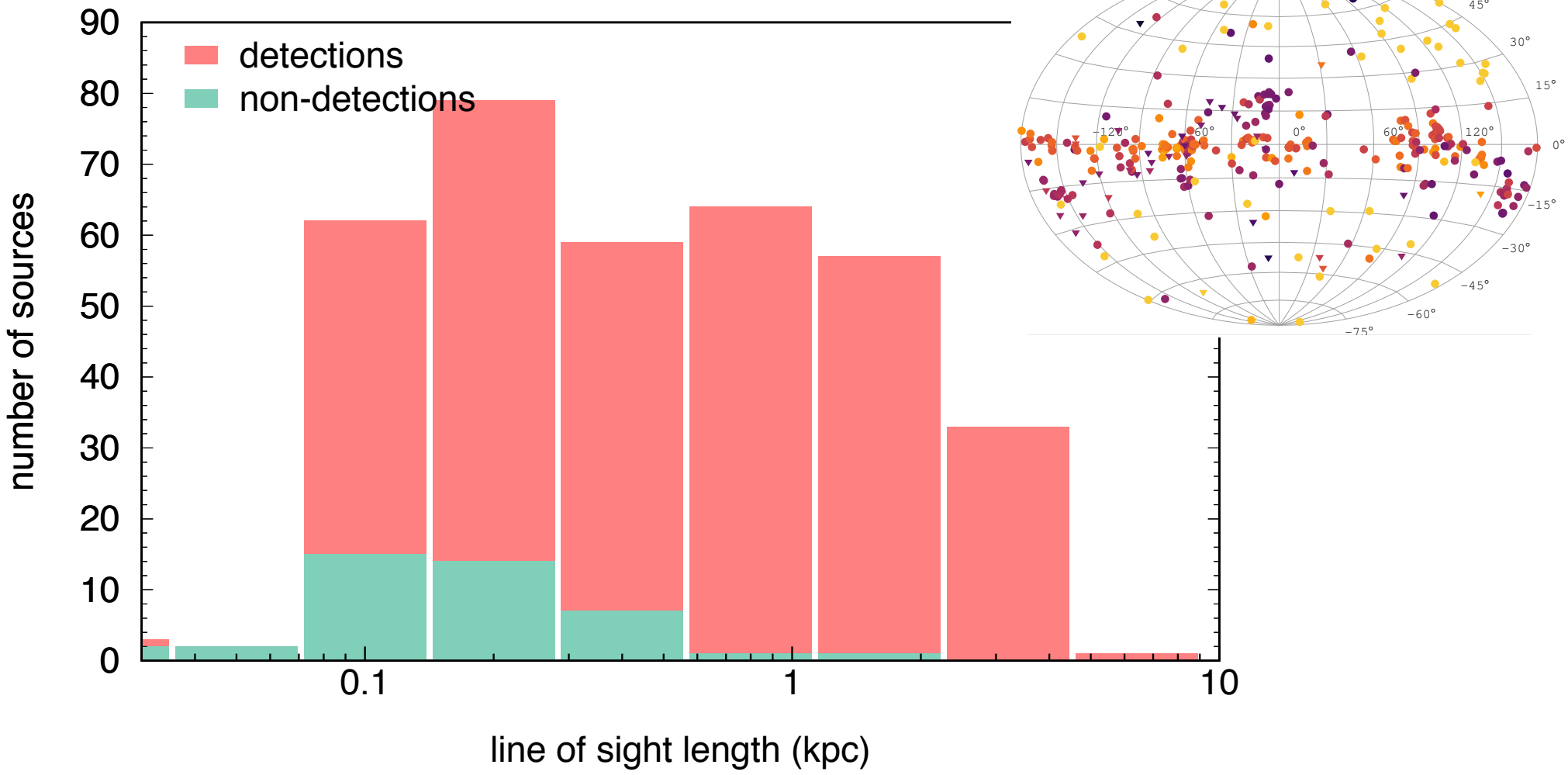

360 lines of sight ⟶

- 312 detections of H_2
- 48 upper limits

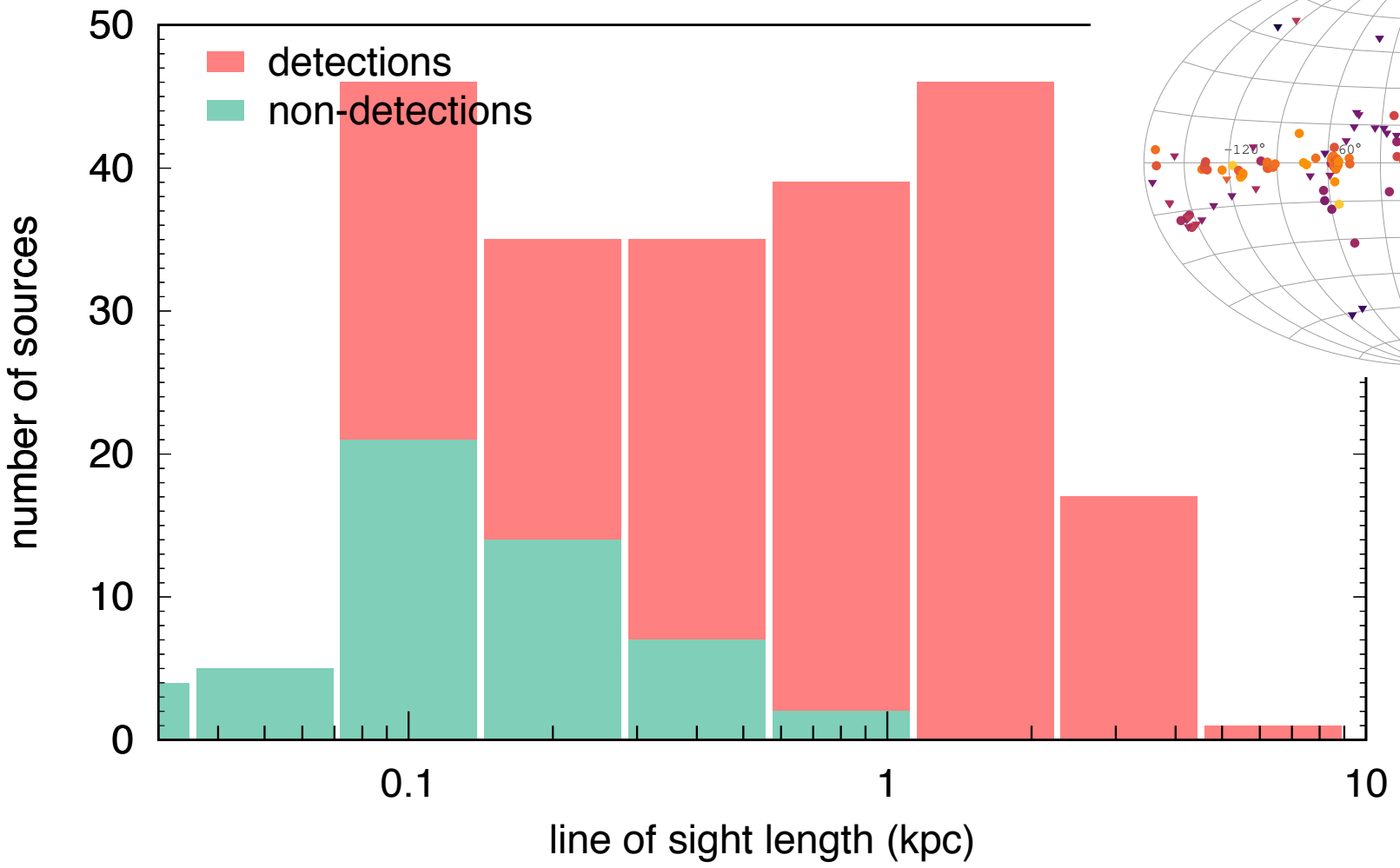

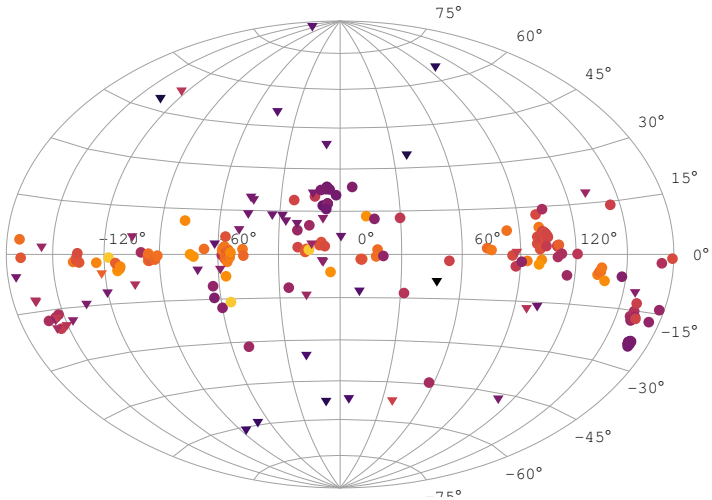

229 lines of sight ⟶

- 175 detections of CH^+
- 54 upper limits

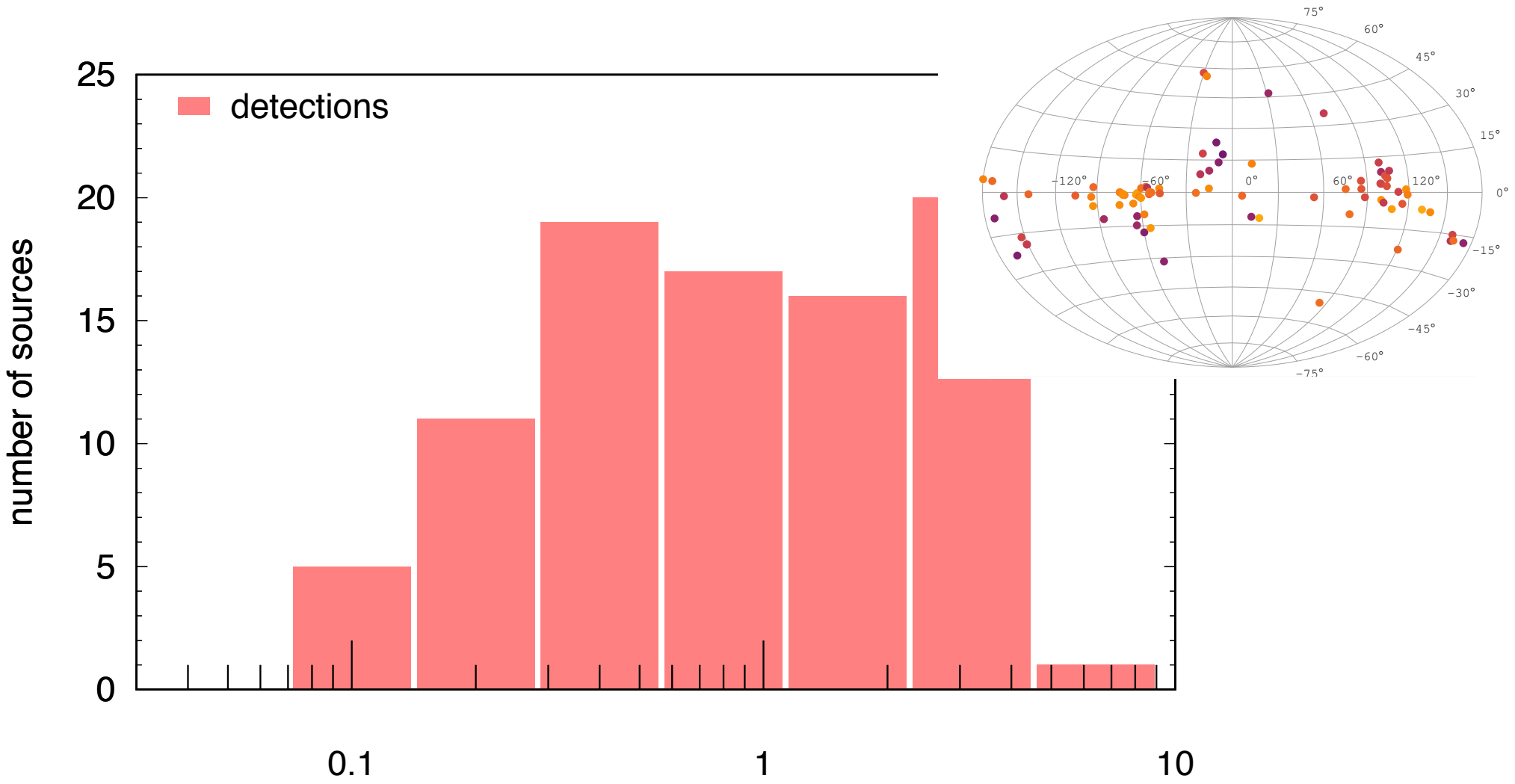

89 lines of sight

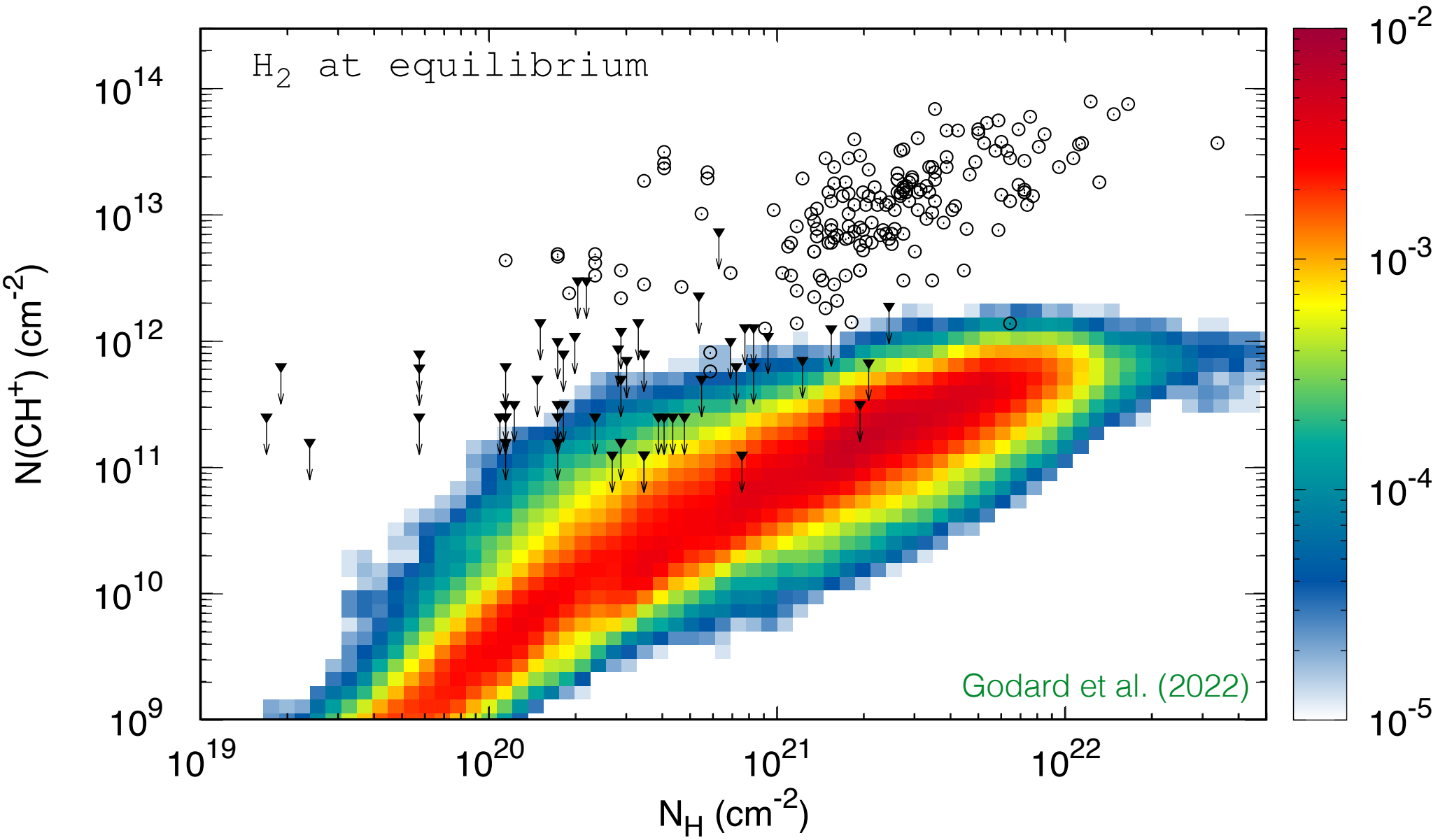
H2 at equilibrium
N(CH+) (cm-2)
NH (cm-2)
Godard et al. (2022)

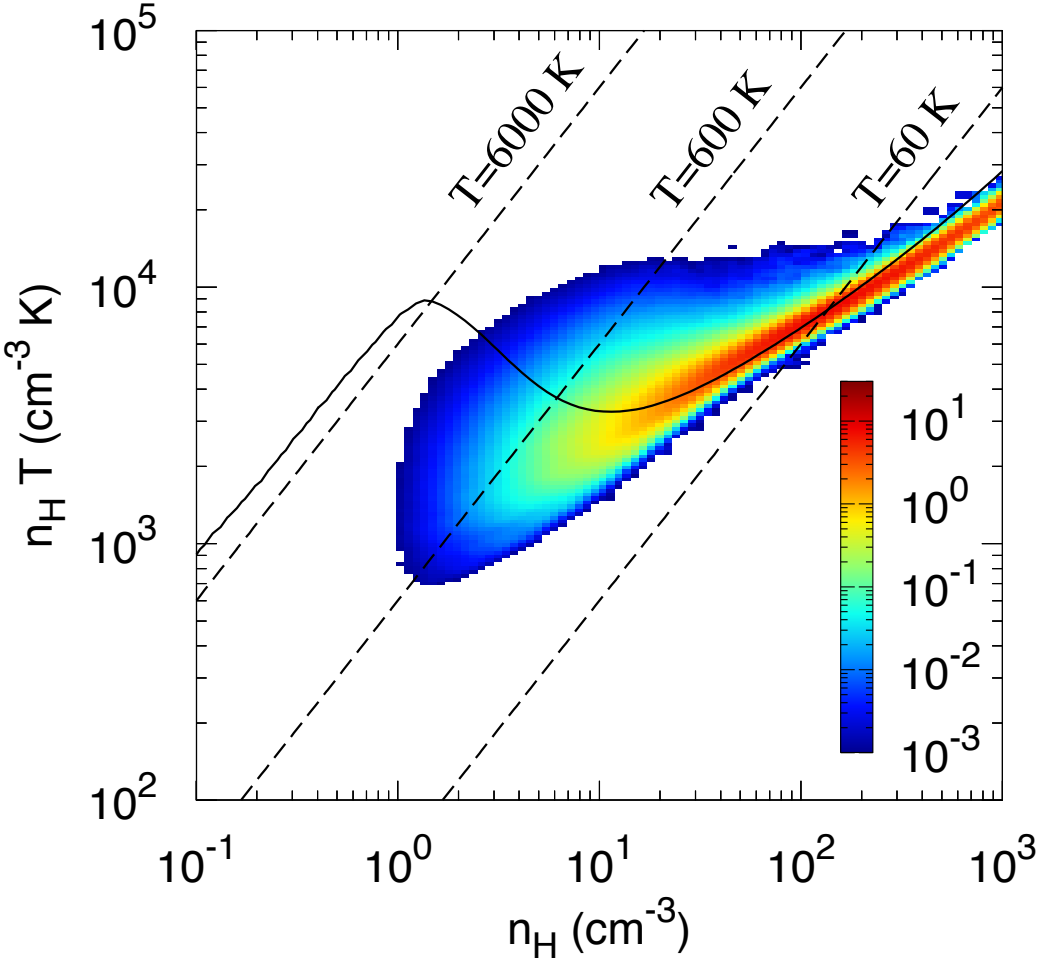

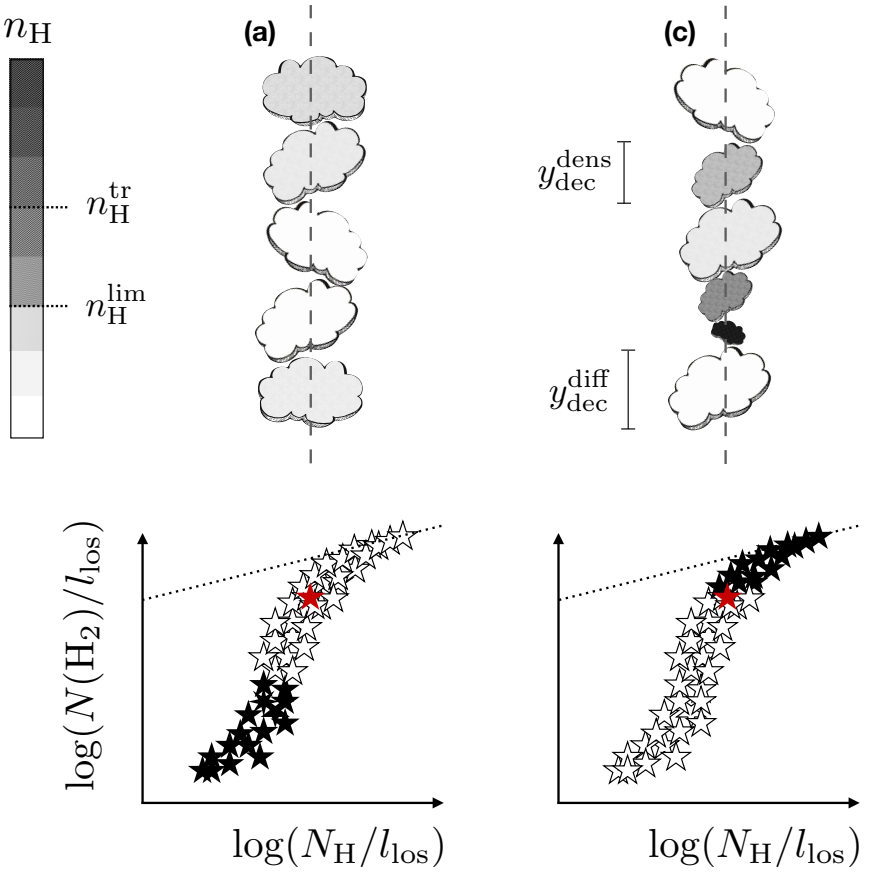

Bellomi et al. (2020)

→ mass of H_2 formed in the CNM

→ distribution depends on the mass and volume of phases

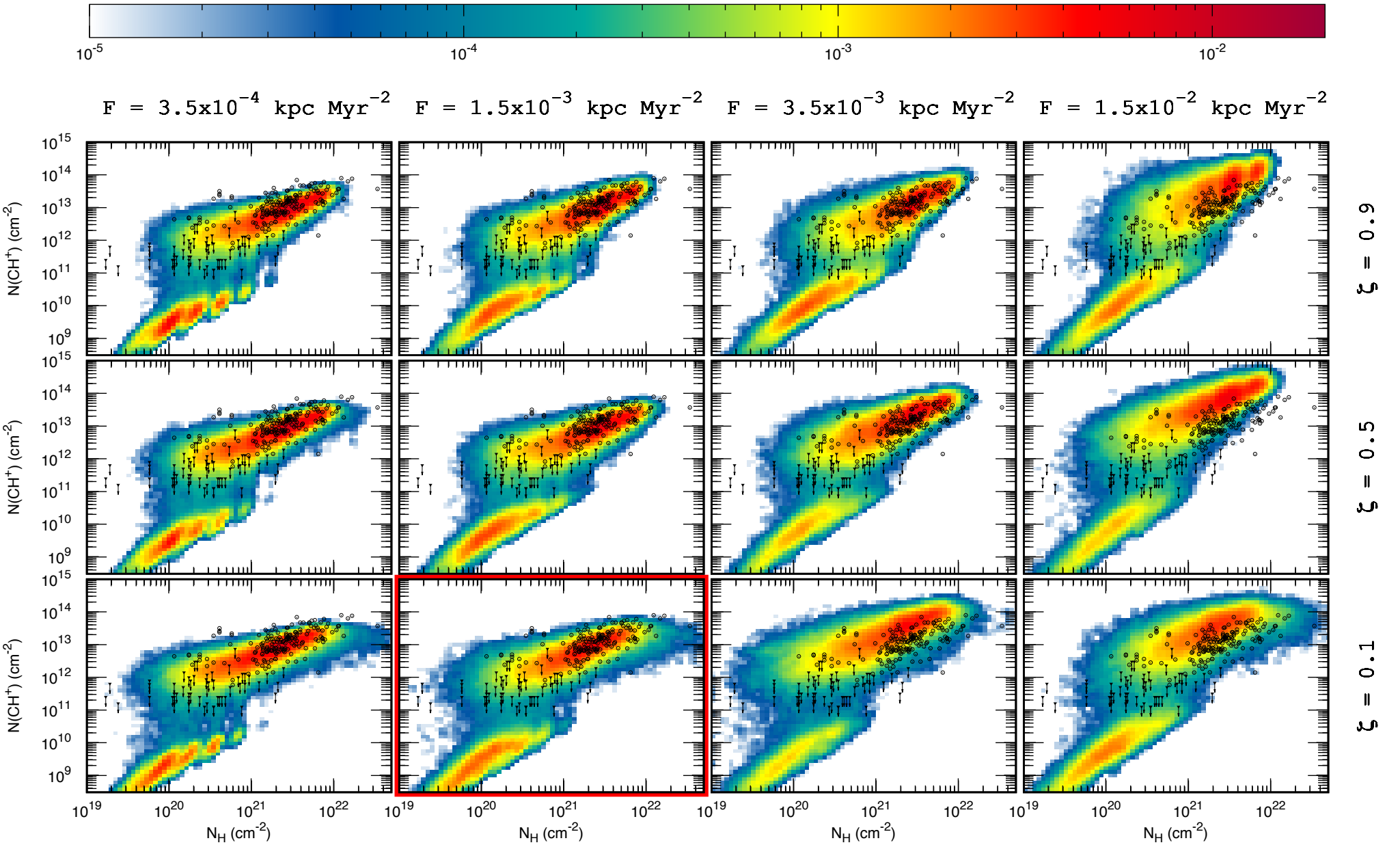
10^-5
10^-4
10^-3
10^-2
F = 3.5x10^-4 kpc Myr^-2
F = 1.5x10^-3 kpc Myr^-2
F = 3.5x10^-3 kpc Myr^-2
F = 1.5x10^-2 kpc Myr^-2
N(CH+) (cm-2)
NH (cm-2)
ζ = 0.9
ζ = 0.5
ζ = 0.1

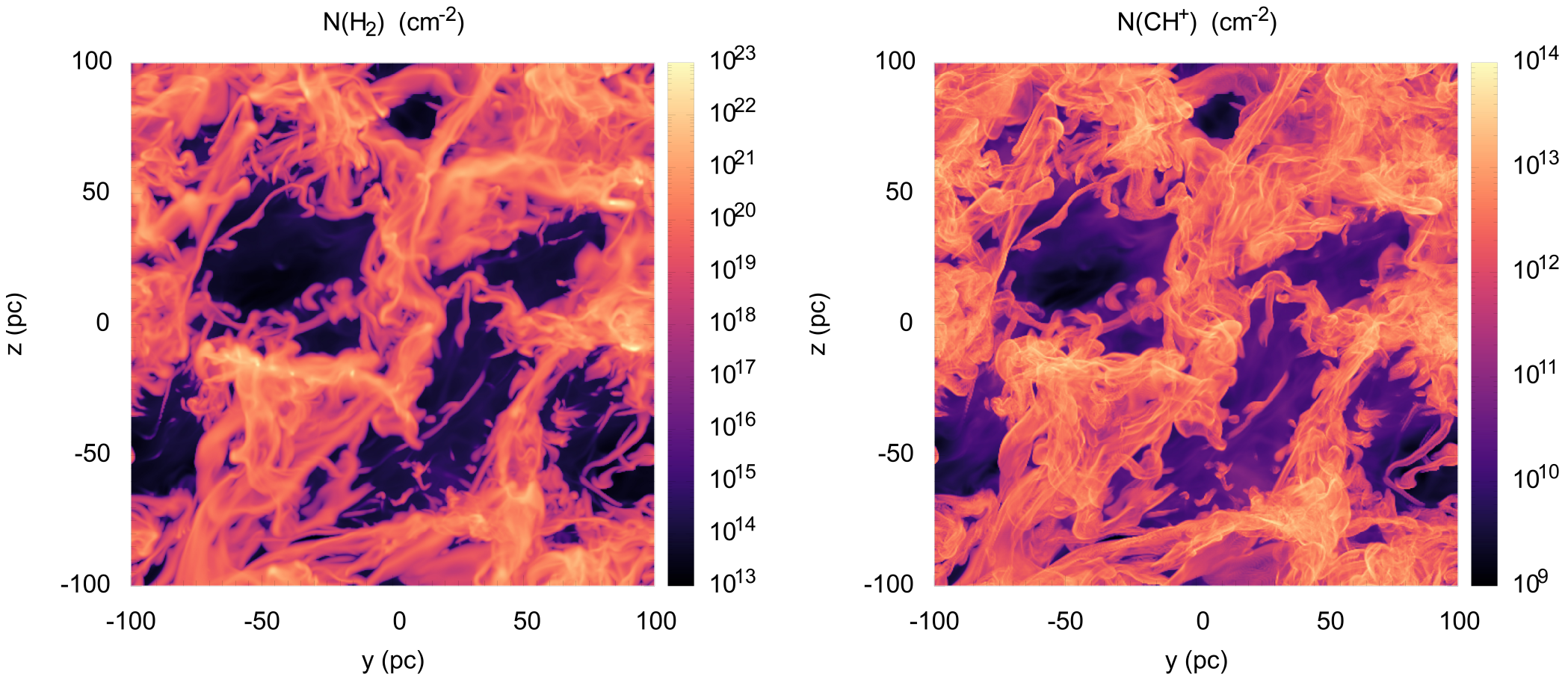
N(H2) (cm-2)
100
50
0
-50
-100
z (pc)
-100
-50
0
50
100
y (pc)
10^23
10^22
10^21
10^20
10^19
10^18
10^17
10^16
10^15
10^14
10^13
N(CH+) (cm-2)
100
50
0
-50
-100
z (pc)
-100
-50
0
50
100
y (pc)
10^14
10^13
10^12
10^11
10^10
10^9

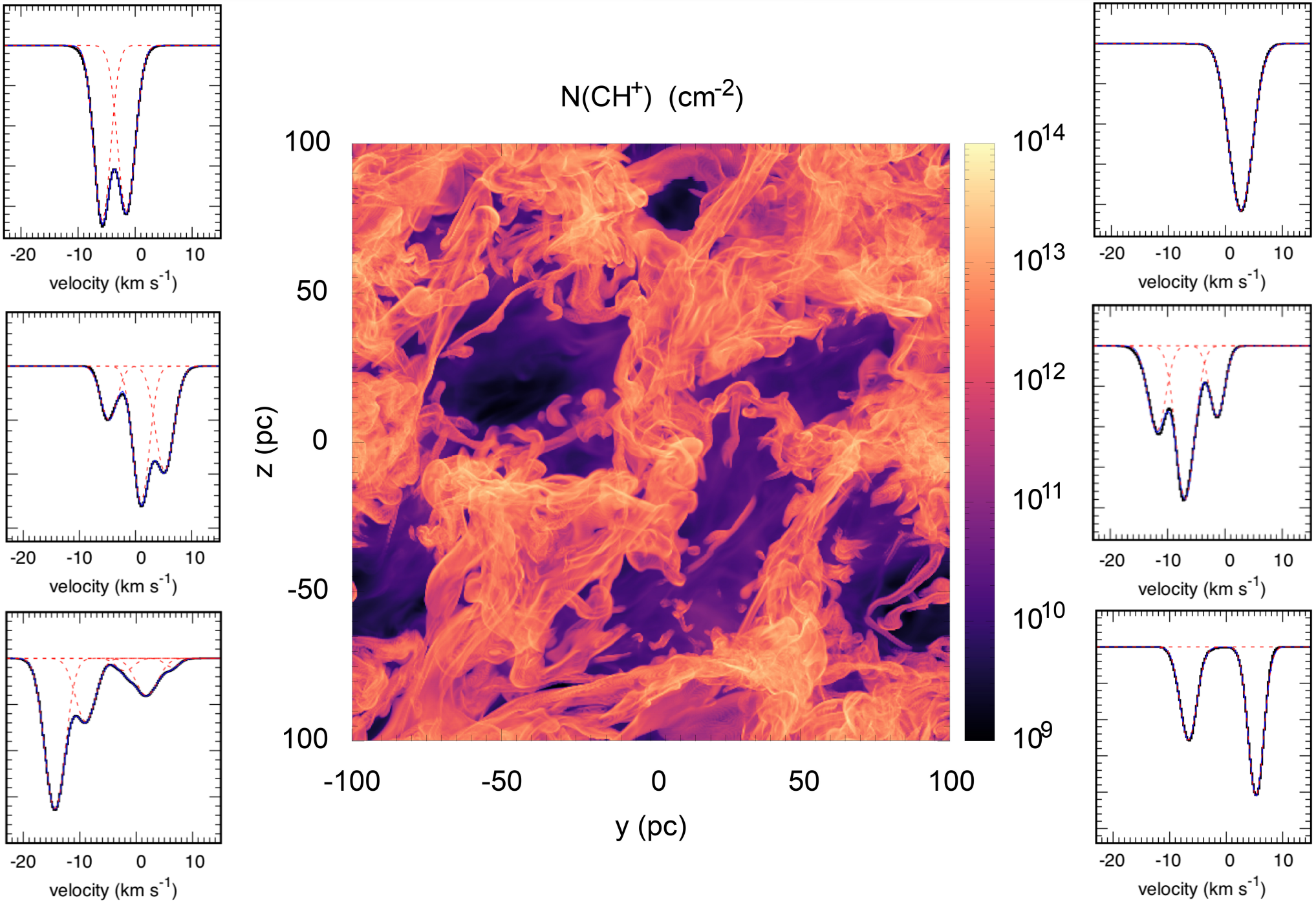
N(CH+) (cm-2)
z (pc)
y (pc)
100
50
0
-50
100
-100
-50
0
50
100
10^14
10^13
10^12
10^11
10^10
10^9
-20
-10
0
10
velocity (km s-1)

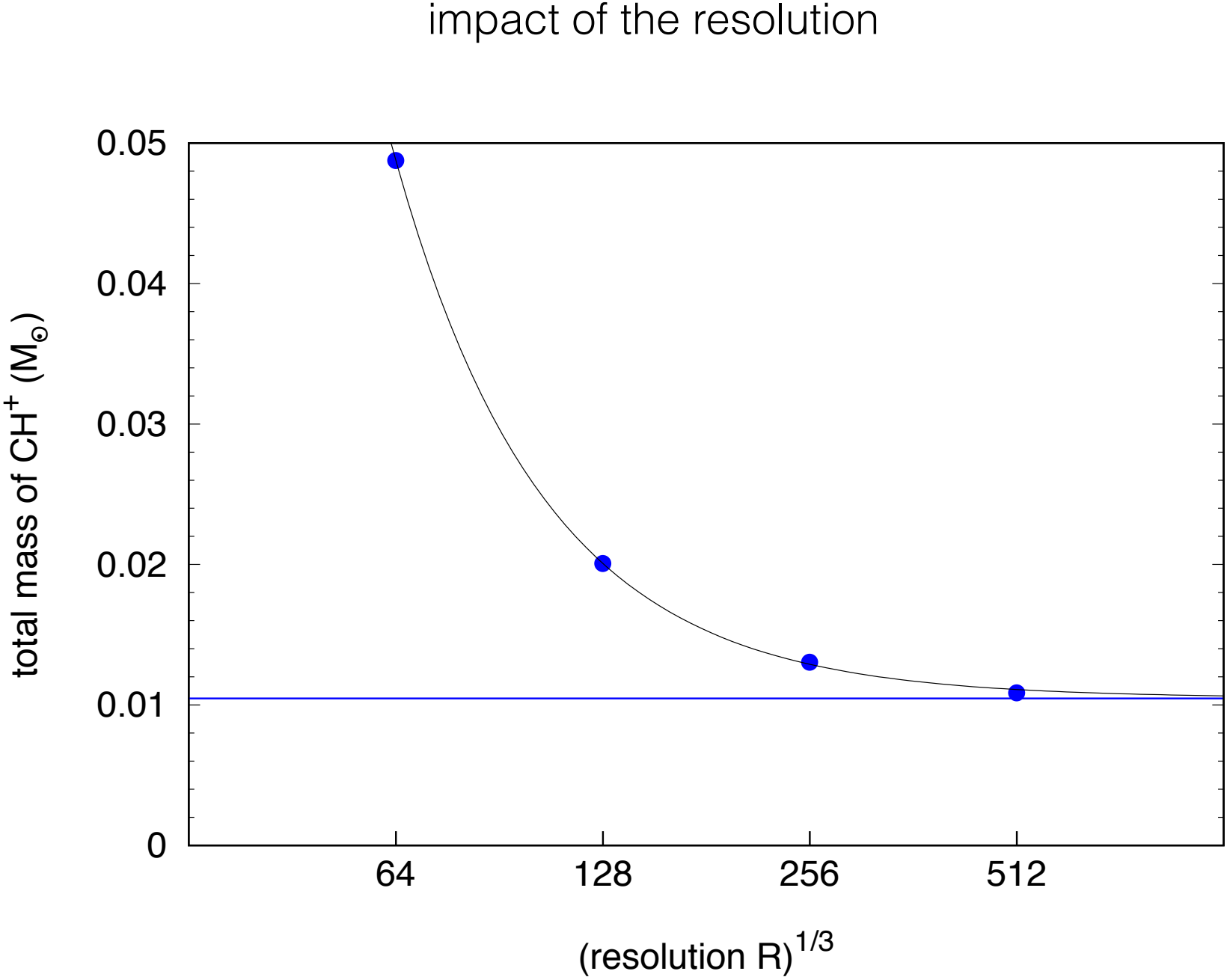
impact of the resolution
0.05
0.04
0.03
0.02
0.01
0
total mass of CH+ (M⊙)
64
128
256
512
(resolution R)1/3

impact of the resolution